Mechanical and Biochemical Properties of Human Cervical Tissue

by

Kristin M. Myers

University of Michigan (2002)
Submitted to the Department of Mechanical Engineering
in partial fulfillment of the requirements for the degree of

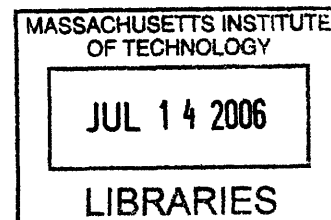Master of Science in Mechanical Engineering

at the

MASSACHUSETTS INSTITUTE OF TECHNOLOGY

January 2005
[February 2005]

Signature of Author . . . .
Department of Mechanical Engineering
January 15, 2005

Certified by . . . .
Simona Socrate
Assistant Professor of Mechanical Engineering
Thesis Supervisor

Accepted by . . . .
Anand
Professor of Mechanical Engineering
Chairman, Department Committee on Graduate Students

Mechanical and Biochemical Properties of Human Cervical Tissue

by

Kristin M. Myers

Submitted to the Department of Mechanical Engineering
on January 15, 2005, in partial fulfillment of the
requirements for the degree of
Master of Science in Mechanical Engineering

Abstract

The mechanical integrity of cervical tissue is crucial for maintaining a healthy gestation. Altered tissue biochemistry can cause drastic changes in the mechanical properties of the cervix and contribute to premature cervical dilation and delivery. This work presents an investigation of the mechanical and biochemical properties of cervical samples from human hysterectomy specimens. Three clinical cases were investigated: non-pregnant hysterectomy patients with previous vaginal deliveries, non-pregnant hysterectomy patients with no previous vaginal deliveries, and pregnant hysterectomy patients at time of cesarean section. Tissue samples for the three clinical cases were tested mechanically and analyzed for biochemical content. Tissue samples were tested in confined and unconfined compression, and biochemical assays measured cervical tissue hydration, collagen content, collagen extractability, and sulfated glycosaminoglycan content. The non-pregnant tissue was found to be significantly stiffer than the pregnant tissue. Collagen extractability was significantly higher in the pregnant tissue. This study represents a first important step towards the attainment of an improved understanding of the complex interplay between the molecular structure of cervical tissue and its macroscopic mechanical properties.

Thesis Supervisor: Simona Socrate
Title: Assistant Professor of Mechanical Engineering

Contents

Chapter 1

Literature Review

1.1 Cervical Insufficiency: Clinical Introduction

The cervix is a dense fibrous organ located at the lower end of the uterus which acts as a mechanical barrier to retain the fetus during pregnancy. Figure 1-1 illustrates the location of the cervix in the female pelvic region during pregnancy. The cervix remains firm until the fetus reaches term around 38 weeks. Then, at time of delivery, the cervical tissue softens and dilates to allow the baby passage. The process of cervical softening is called maturation, and it begins with a biochemical cascade of events triggered by hormonal change. These events prepare the body for vaginal delivery of the fetus, and are characterized by drastic remodelling of the cervical tissue. A premature onset of these conditions can lead to pre-term delivery. Pre-term delivery is usually defined as birth before 28 weeks gestational age.

Pre-term delivery associated with a contraction-free, gradual cervical dilation, and spontaneous delivery during mid second trimester to early third trimester is called cervical insufficiency. Cervical insufficiency is an asymptomatic condition in which the patient can be unaware of the condition until time of spontaneous delivery.

Cervical funneling and fetal membrane prolapse are two signals of pre-term birth associated with cervical insufficiency. Cervical funneling is characterized by a T, Y, V, U pattern of progressive cervical deformation which can be observed by ultrasound and Magnetic Resonance Imaging [10]. Figure 1-2 is a diagram of the cervical funneling pattern. Membrane prolapse is characterized by "hourglassing" of the fetal membrane into the vaginal canal. "Hourglassing"

Fetus in Utero

placenta

umbilical cord

uterus

cervix

fetus

amniotic sac
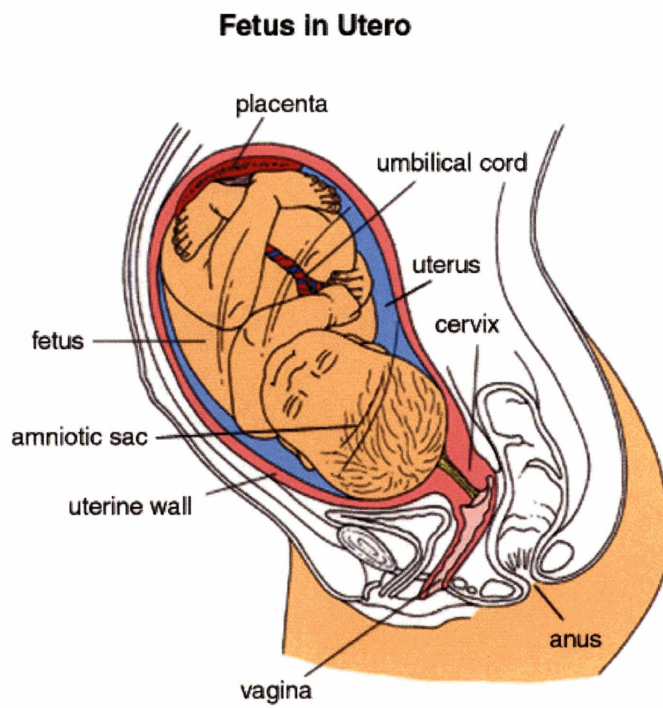
uterine wall

anus

vagina

Figure 1-1: Female pelvic region during pregnancy. The cervix is the lower region of the uterus which acts as a mechanical barrier during pregnancy to keep the fetus within the uterus.

©2001 Philippe Jeanty
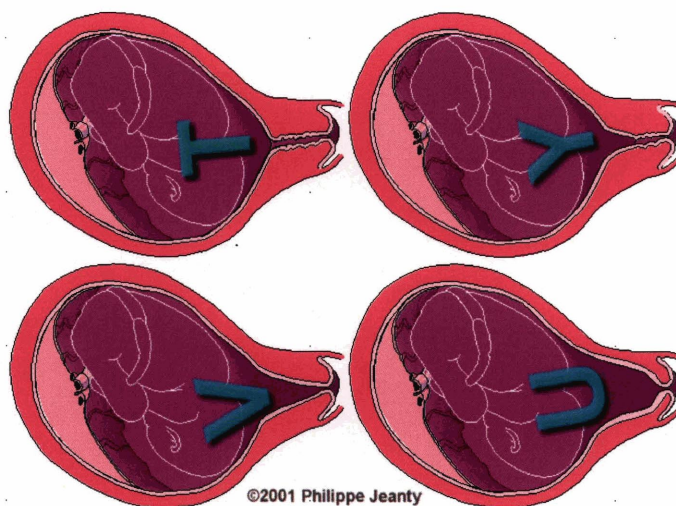
Figure 1-2: T,Y,V, and U cervical dilation pattern during cervical funneling.

refers to the shape of the fetal membrane as it slips into the inner cervical canal and bulges into the vaginal canal. Figure 1-3 shows bulging membranes observed during vaginal examination in a patient with cervical insufficiency. Typically, the progression of labor is difficult to stop with the onset of funneling and prolapse.

Despite increases in prenatal care the rate of pre-term birth has increased in the past years. In the United States, the rate of pre-term birth has increased from 9.5% to 12% in the past 20 years[21]. Preterm birth is one of the leading causes of morbidity and mortality in newborn infants, and cervical insufficiency is estimated to cause approximately 15% of pre-term birth. Regardless of the low occurrence of pre-term birth associated with cervical insufficiency, this condition is of substantial medical relevance because it is associated with extremely premature deliveries. The survival rate of the baby is directly dependent on its gestational age. Survival increases from 5% for babies born at 23 weeks to more than 95% by week 32 [64][57]. Therefore, deliveries associated with cervical insufficiency typically result in newborn death or severe neurological abnormalities. The impact of cervical insufficiency remain unknown because criteria for a conclusive diagnosis are still controversial.

Figure 1-3: Membrane prolapse into vaginal canal.

1.1.1 Diagnosis

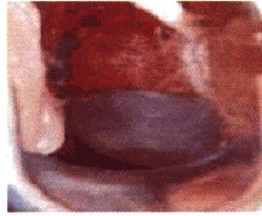Cervical insufficiency is typically diagnosed when funneling and protruding membranes are clinically observed. At the time of this diagnosis, it is generally too late to stop the progression of pre-term labor associated with cervical insufficiency. Cervical insufficiency is different from other causes of pre-term labor such as pre-term ruptured membranes, bleeding, and intraamniotic infection in that its degree of severity is a continuous variable spanning a wide range of conditions [31]. The severity of cervical insufficiency is dependent on a combination of congenital, anatomical, obstetric, and biochemical factors. In an attempt to develop an early diagnostic tool researchers have suggested that cervical insufficiency may be identified from a combination of these factors.

A recent report by Goldenberg et al. in 2003 outlined several risk factors associated with pre-term birth. The report reached conclusions based on the The Pre-term Prediction Study conducted by the Maternal Fetal Medicine Network between 1993 and 1996 [21]. The study surveyed risk factors for pre-term birth in over 3,000 women at 10 centers. The monitored risk factors include obstetric history as well as clinical findings of the current pregnancy. Results of the Pre-term Prediction Study indicate that the three most important risk factors associated with cervical insufficiency are cervical/vaginal fetal fibronectin concentration during current pregnancy, history of pre-term birth, and short cervical length. Table 1.1 outlines these risk factors and their associated odds ratios. The odds ratio is the odds in favor of the condition for the experimental group divided by odds in favor of the condition for the control group. Fetal fibronectin had the highest odds ratio. The relative risk of pre-term birth doubles with increasing values of fetal fibronectin from 20-40ng/ml to 60-90ng/ml [21].

9

Risk Factor	Test Cutoff	Odds Ratio for < 32 weeks	Odds Ratio for < 35 weeks
Fetal Fibronectin Level	≥50ng/ml	32.7	9.1
Short Cervix	< 25mm	5.8	5.5
Previous Spontaneous Pre-term Birth	Positive	4.5	4.3.

Table 1.1: Risk Factors for spontaneous preterm delivery before 32 and 35 weeks gestation assessed by the Preterm Prdiction Study (Iams et al.)

Obstetric History

Known obstetric history risk factors associated with cervical insufficiency are [21]:

- History of previous pre-term birth before 28 weeks

- Cervical injury from previous late surgical termination of pregnancy

- Cervical injury from obstetrical cervical lacerations

- Cervical injury from extensive conization procedures

- High fetal fibronectin level during pregnancy

One of the major risk factors for pre-term birth is a history of previous pre-term birth. The risk of future pre-term birth increases as the number of previous pre-term birth increases. The subsequent risk also increases with decreasing gestational age of the prior birth. For example, there is a 10-fold increase in having a subsequent pre-term birth if the previous pre-term birth was less than 28 weeks gestation, and there is a 22-fold increase in pre-term birth for those women who had a previous pre-term birth between 23 and 28 weeks of gestation [21].

Clinical findings for the current pregnancy

Clinical findings for the current pregnancy that are most often associated with cervical insufficiency are:

- Multiple gestation

- Excessive uterine volume

- Abnormal anatomical factors

Abnormal anatomical factors are most commonly identified by the following measurements: cervical length, cervical funnel width and length, percent funneling and cervical dilation index [23]. Sonographic imagining during a routine pelvic exam is used to identify and measure these factors. Two statistical cohort studies by Iams et al. and Guzman et al. found a correlation between cervical canal length and cervical insufficiency. These research groups performed studies on groups of women with previous pre-term births and women with normal previous pregnancies. Iams et al. conducted an early cross-sectional study of women with previous pre-term birth before 26 weeks, pre-term birth at 27 to 32 weeks, pre-term birth at 33 to 35 weeks, and women with normal obstetric history. This study identified a direct correlation between the gestational age of the previous pre-term delivery and cervical length such that earlier deliveries were typically associated with shorter cervical length [31]. Guzman et al. conducted a retrospective cohort study on women with normal and abnormal obstetric histories. The study investigated the cervical lengths of the women's current pregnancy between 15 and 20 weeks and between 21 and 24 weeks gestation. Guzman et al. also concluded that the gestational age of the prior delivery could be directly correlated to the length of the cervical canal during the current pregnancy [22].

Guzman et al. also investigated if a different set of anatomical factors funnel width and length, cervical length, percent funneling and cervical index were better predictors for pre-term labor. A cohort of 496 high risk patients were evaluated between 15 and 24 weeks gestations and followed to the end of pregnancy. Investigators found that each parameter did equally well in predicting the outcome of pre-term birth. They recommended that cervical length was a good predictor of spontaneous pre-term births because it was the easiest to measure with reasonably low error. Based on the results of this study, Guzman et al. recommended bed rest and possible cerclage for women with cervical lengths between 2.0cm and 1.6cm and cerclage placement for cervical length below 1.6cm. Further, they cautioned that cervical length as a predictor is strongly influenced by obstetric risk factors such as prior spontaneous pre-term birth. The investigators cited high sensitivity, specificity and negative predictive value for the cervical length diagnostic test. However, the positive predictive values were extremely low. The positive predictive value is the probability that the women will develop the condition given positive test result. Because of this statistical discrepancy and the difficulty in measuring
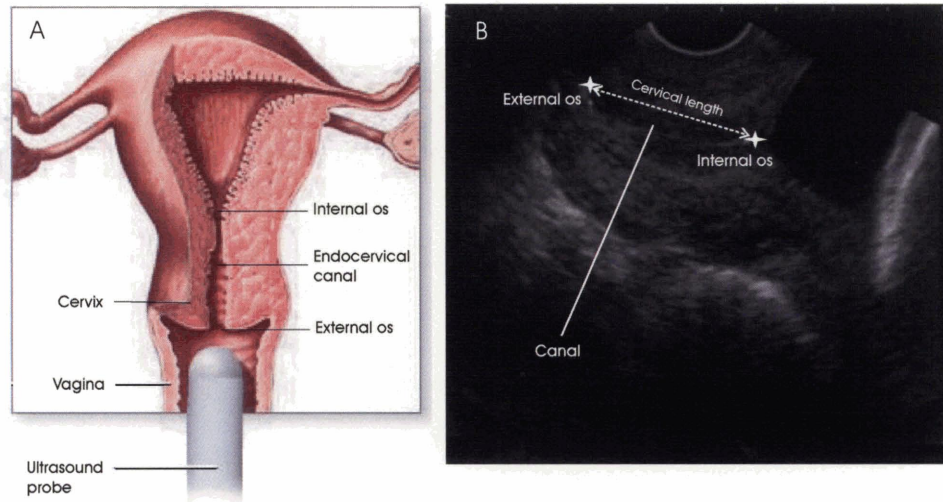
Figure 1-4: A) Illustration of the ultrasound probe location in the vagina. B) Image of the cervix and the defination of the cervical length measured on the image.

congenital factors, this diagnosis criterion is still controversial [23].

1.1.2 Prevention and Treatment

Preventive measures for preterm birth associated with cervical insufficiency are bed rest, cerclage, and pessary. They are prescribed according to the severity of the individual patient's condition. The most prescribed measures are bed rest and cerclage. Cerclage is a suture stitch used to tie the cervix closed. Bed rest is a non-surgical solution to prevent further cervical funneling. In extreme situations the patient is inclined at a negative angle. A more invasive treatment option is to surgically place a transvaginal or transabdominal cerclage.

Transvaginal cerclage is used for women with a history of cervical insufficiency (preventive cerclage) or women with a current presentation of cervical insufficiency. A cerclage is never placed in patients with active labor, cervical anomalies, intrauterine infection or premature rupture of membranes (PROM). Preventive cerclage is typically placed at 13-14 weeks gestation, and is performed vaginally. See Figure 1-5 for an illustration of a transvaginal cerclage. The two types of transvaginal cerclage are the McDonald and Shirodkar Procedure. The McDonald Procedure uses a 5mm thick non-dissolvable suture material which is weaved through the cervix and tied off. The Shirodkar is similar, however, it is placed closer to the uterus and it is weaved
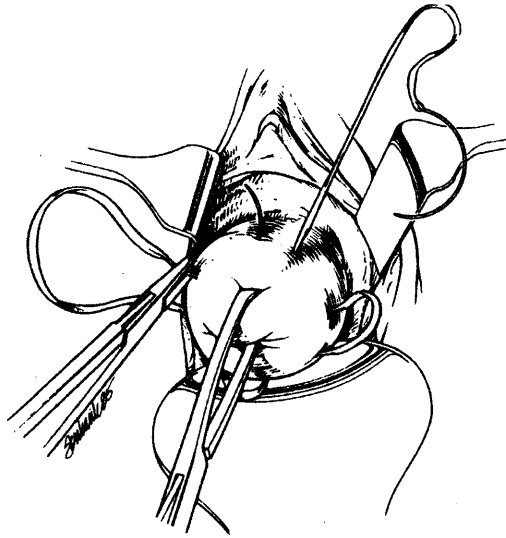
12

Figure 1-5: Surgical procedure for transvaginal cerclage.

under the skin then pulled tight to shut the cervical canal. This procedure can be used with a short cervix, however it is more difficult to place and more difficult to remove. The success rates for both procedures are not significantly different. McDonald procedure success rate is 63-89%, and the Shirodkar procedure success rate is 75-85% [5].

Transabdominal cerclage is used for women with previous failed transvaginal cerclage and for women whose cervix is too short for vaginal cerclage. As illustrated in Figure 1-6, the cervix is accessed through the abdomen and it is sewn closed at the internal OS. This stitch is higher than the transvaginal stitches and it requires cesarean section delivery. This method has a reported higher success rate of 82-100% [47]. However, it requires major abdominal surgery with complications including hemorrhage, infection, fetal loss, and PROM.

The effectiveness of the cerclage procedure is unclear because diagnostic criteria for cervical insufficiency are still controversial. Three observational studies [4][26][28]and two randomized trials [1][58] assess cerclage procedures. Results from these studies reach conflicting conclusions. Two of the observational studies, Heath et al. [26] and Hibbard et al. [28] found pre-term birth before 34 weeks was statistically lower in the cerclage group. On the other hand, the third observational study, Berghella et al. [4], found no statistical difference between the cerclage
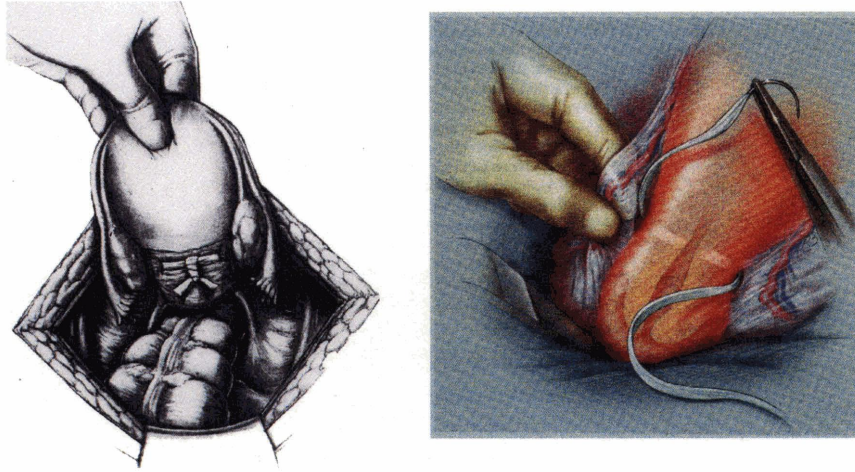
Figure 1-6: Surgical procedure for transabdominal cerclage.

and control groups.

Althuisius et al. and Rust et al. conducted prospective randomization studies to assess the effectiveness of cerclage procedures and reached opposite conclusions. Althuisius et al. [1] claimed that cerclage is an effective treatment for women at risk of cervical insufficiency. The group defined high risk patients as women with previous pre-term delivery before 34 weeks of gestation, previous pre-term rupture of membranes before 32 weeks of gestation, history of cold knife conization, diethylstilbestrol exposure, uterine anomaly, or cervical length below 2.5cm before 27 weeks of gestation. The high risk patients were randomized into two groups: the cerclage and the bed rest groups. The cerclage group received a single purse-string suture and prescribed bed rest. The bed rest group received bed rest only. The cerclage group had significantly lower pre-term delivery before 34 weeks and significantly lower compound neonatal morbidity (neonatal morbidity is admission to the neonatal intensive care unit or neonatal death) [1].

On the other hand, Rust et al. [58] concluded that there is no benefit to cerclage therapy. Their study randomized 135 patients into two groups, a cerclage group and a no-cerclage group.

Women included in the study were between 16 and 24 weeks gestation and showed the following signs of cervical insufficiency: a short cervix below 25mm, internal os dilation, or membrane prolapse into the cervical canal at least 25% of the cervical length [58].

The difference in study design may contribute to the conflicting results between Rust et al. and Althuisius et al. The two groups used different criteria of inclusion for their randomized trials. Rust et al. included women with prolapsing membranes, but Althuisius et al. did not include women with prolapsing membranes. Further, Althuisius et al. only had 35 women in their study while Rust et al. included 113 patients. These conflicting results highlight the need to improve our understanding of the mechanisms leading to cervical insufficiency.

1.2 Biochemical Characteristics of Cervical Tissue

The cervix has two distinct functions during pregnancy. First, it must remain firm and closed during the length of pregnancy to retain the fetus. Second, it must soften dramatically to allow delivery at term, normally around 38 weeks of gestation. Cervical insufficiency is associated with the premature delivery of the fetus because of the premature "softness" of the cervix. This "softness" is related to an altered biochemical content of the tissue which include collagen, water, proteoglycans, and glycosaminoglycans.

This section reviews the biochemical literature relating to pregnant, non-pregnant and insufficient cervix. Each biochemical component is introduced with a brief explanation of its structure. Then each component's function and its possible role in determining the mechanical properties of the tissue are discussed.

1.2.1 Extracellular Matrix Components of Cervical Tissue

Cervical tissue is primarily composed of a dense insoluble extracellular matrix (ECM). The cellular component is typically below 5-10% per weight [59]. The ECM provides strength and rigidity to resist mechanical loading, and provides a scaffold for cell attachment and migration. The biochemical constituents of the ECM are tissue and function specific. The constituents of cervical ECM include a three dimensional collagen network embedded in a highly viscous groundsubstance. The collagen network contains highly crosslinked type I and III fibrils, and
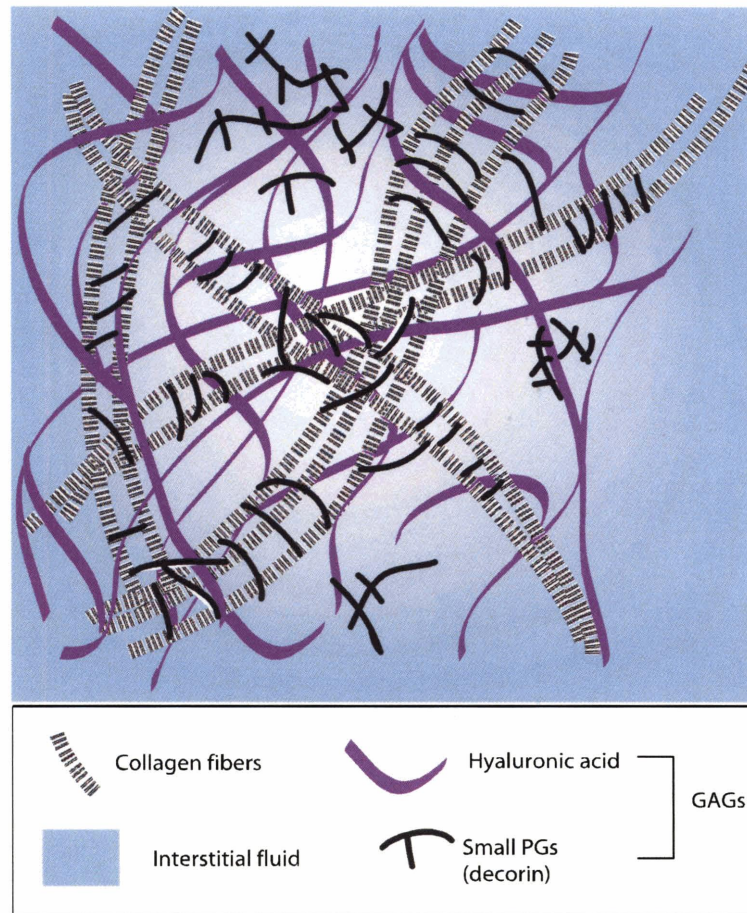
Figure 1-7: The extracellular matrix of the cervix is composed of a three-dimenstional collagen fibril network containing type I and III fibrils. Surrounding the collagen network are proteoglycans, glycosaminoglycans, and interstitial fluid.

the groundsubstance is composed of interstitial fluid, proteoglycans (PGs) and glycosaminoglycans (GAGs). The glycosaminoglycans are present either in the form of proteoglycans such as dermatan sulfate in decorin, or they are embedded in the matrix without a core protein as in the case of hyaluronic acid. The ECM supports cervical cells, mainly fibroblasts and a small amount of muscle cells. Figure 1-7 represents the biochemical constituents of the cervical ECM. See Table 1.2 below for the percentage of each constituent [38].

Cervical maturation is independent of uterine activities, and is associated with cervical tissue remodelling. Leppert and Garfield et al. have summarized cervical conditioning as an inflammatory cascade of events which is triggered by hormonal changes [42][19]. This process

Water	80%				
Dry tissue	20%				
	Collagen ~70% [41]	GAGs ~0.2% ([55], [54])			Elastin ~2% [45]
	Type I Type III	Dermatan sulfate	Heparan sulfate	Hyaluronic acid	
	~70% ~30% ([37], [32])	76%	13% [65]	11%	

Table 1.2: Main constituents of human cervical tissue in non-pregnant women (Febvay [17])

includes:

- Release of proinflammatory cytokines

- Migration of white blood cells to the cervical tissue

- Release and activation of degradative enzymes such as matrix metalloproteinases

- Increase in collagen and glycoprotein turnover and synthesis

- Disruption of collagen network superstructure

- Change in decorin and collagen ratio

- Increase in hyaluronic acid concentration

- Increase in interfibrillar fluid

Studies on both human and animal models have examined cervical softening at different stages of pregnancy. Shimizu et al. analyzed human biopsy samples for glycosaminoglycan content and its related biochemical alterations at different gestation periods [61]. Kokenyesi and Woessner studied dermatan sulfate levels related to mechanical creep properties of rat cervix at different gestational age [40]. Danforth and Ekman investigated the collagen solubility of human biopsy specimens in a variety of solvents to measure the strength of collagen cross-linking. This study also measured hydration and collagen concentration levels for non-pregnant and at term human cervical specimens [11]. Substantial differences in methods and protocols to test and prepare cervical tissue result in large discrepancies in the results of these studies. Therefore, conflicting mechanical and biochemical data exist in the literature.

1.2.2 Water Content

Danforth et al. measured the hydration levels in human post partum and non-pregnant cervix. They found a slight increase from 74.4% to 78.4% in water content from the nonpregnant to the post partum cervix [11]. Shimizu et al. also found that water content in human cervix was higher in postpartum than in non-pregnant tissue. The water content was 78.1%, 79.7%, and 83.6% for proliferative phase nonpregnant, secretory phase nonpregnant, and post partum cervix, respectively [61].

1.2.3 Collagen

Collagen Synthesis and Structure

Collagen is the most abundant protein in humans and exists in at least 20 different forms. Different forms appear in various organs and tissues depending on their function. The extracellular matrix of load-bearing soft tissue contains a high percentage of fibril collagen with strong tensile strength. The fibril collagen types are mainly type I, II, and III, and they are insoluble in solvents which disrupt ionic interactions and hydrogen bonding [66]. In the cervix, collagen accounts for 85% of dry mass with 70% type I and 30% type III fibrils [15].

Figure 1-8 illustrates the path for collagen fibril and fiber formation. This diagram is specifically for Type I collagen. Type II and III have similar fibril structures. Collagen molecules are first synthesized in the fibroblast rough ER and Golgi Complex. The cell secretes collagen as long procollagen molecules with additional amino acid chains at the N and C terminus. These additional amino acid chains are called the propeptides and believed to be responsible for proper formation of the helical structural. Extracellularly, the propeptides are cleaved through an enzymatic reaction and the collagen molecule becomes tropocollagen which is the basic building block of the collagen fiber[13].

The tropocollagen is approximately 300nm long and 1.5nm thin. It is composed of three coiled peptide chains, two $\alpha 1$ and one $\alpha 2$ chains. The peptide chains have a repeating triplet amino acid sequence of Gly-X-Y. This triplet forms a chain of 1050 amino acids where every third amino acid is glycine. The X and Y can be any amino acid, but most often they are proline and hydroxyproline. The three peptide chains form a right handed helix with three
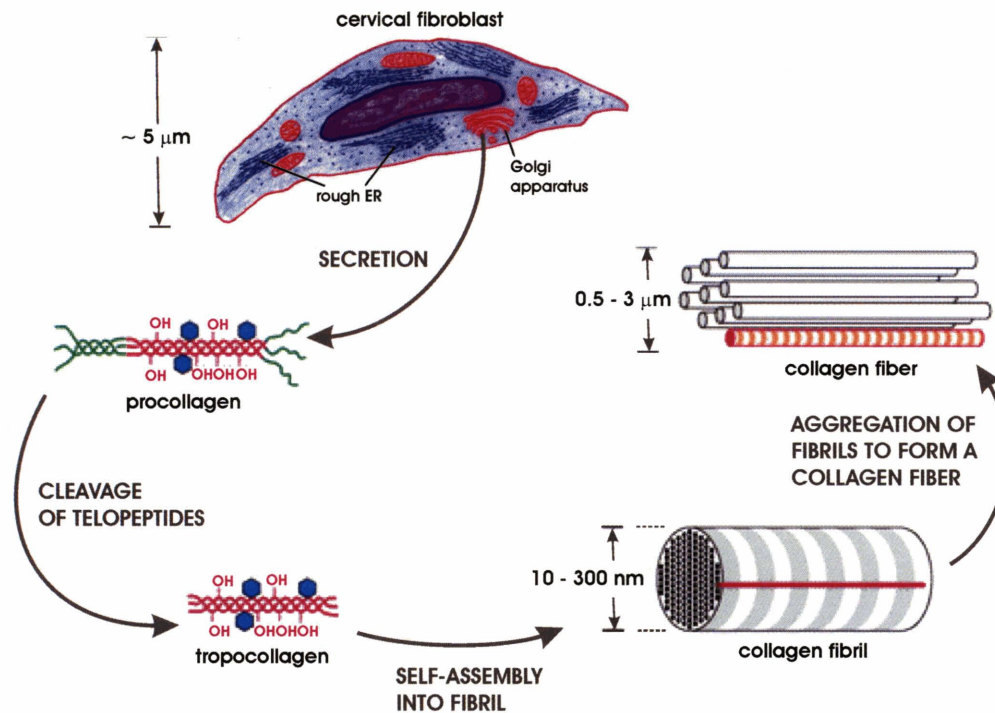
Figure 1-8: Collagen molecules are formed and modifided in a sequence of events which occur in the rough ER, Golgi complex, and the extracellular space. Collagen molecules self aggregate into collagen fibrils which further aggreate to form collagen fibers. (Adapted from Alberts et al, Molecular Biology of the Cell, 3rd ed., Garland Publishing 1994) [18].

amino acids per turn. The space between the peptide chains are only small enough to fit one side chain of glycine. This center location is the site of a strong hydrogen bond between the glycine side chain and a residue from a neighboring amino acid on another chain. This intramolecular bond and the well-packed triple helical structure give the tropocollagen molecule its strong tensile properties.

The tropocollagen self assembles laterally to form the collagen fibril. The tropocollagen pack together in a side-by-side array where every row is displaced by approximately 67nm. Because of this displacement the collagen fibers appear banded in electron micrographs. See Figure 1-9 for fiber and fibril representations. The fibril assembly is driven by spontaneous associations with adjacent collagen molecules and hydrophobic interactions. The fibril assembly is stabilized by covalent cross-links between adjacent tropocollagen molecules. The cross-links are located specifically between the N and C terminus of neighboring molecules, and are formed by an enzymatic reactions located on the lysine and histidine side chains. Up to four side chains can be crosslinked [66] [13].

Once the collagen molecules assemble into fibrils, the fibrils can aggregate into larger "rope-like" fibers. This aggregation of fibrils is tissue and function specific. For example, tendon fibrils are in a parallel bundles optimized to support uniaxial tensile forces. The collagen in skin forms sheets of fibrils which are layered at many angles to withstand biaxial forces [20]. The collagen of articular cartilage can be organized in a three-dimensional anisotropic matrix to support compression forces [6].

Collagen Network Remodelling and Degradation During Pregnancy

Early studies suggest that the remodelling and degradation of the collagen network play a large role in cervical softening [60][48]. In a normal non-pregnant cervix, the collagen fibers are in a tight, organized bundled network. Studies by Aspden et al. [2] found that at term cervical tissue has altered collagen fiber length, alignment, and organization. The collagen fibers become smaller and the collagen network becomes loose and disorganized. The authors claim that the collagen fibers need a critical length of 20μm to maintain tensile strength [2].

Sennstrom et al. argued that there is a distinct inflammatory process that increases the collagenase activity during cervical ripening to cause collagen degradation. The study measured
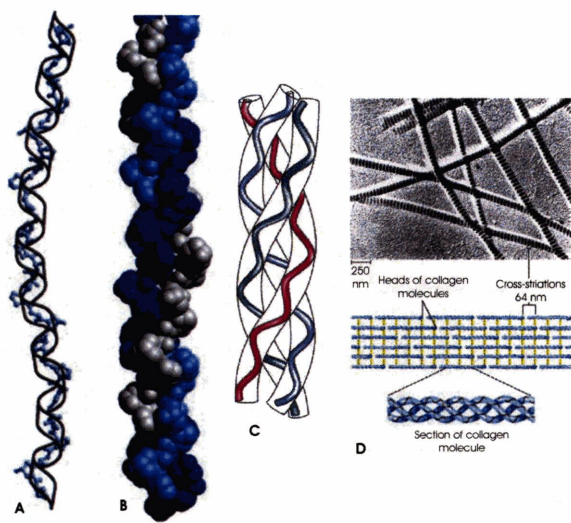
Figure 1-9: A, B, and C are interpretations of the basic tropocollagen molecule. D illustrates the staggered array of the collagen molecule into the fibril formation [18].

increased levels of metalloproteinases (MMP), a collagenase group, in human postpartum cervical samples as compared to nonpregnant cervical samples. Specifically, the levels of MMP-8 for postpartum women was 7300ng/mg wet weight and 86ng/mg wet weight for nonpregnant women. Immunohistochemical stains of nonpregnant and post partum samples confirm increased activity of MMP-8 in the stromal cells of post partum cervix [60]. Another study by Nagase suggests that cervical dilation is associated with the breakdown of collagen fibrils. This study concludes that increased levels of MMPs are associated with cervical softening and maturation [48].

Collagen Network Solubility

The collagen fibrils of the extracellular matrix are intramolecularly and intermolecularly crosslinked. The intramolecular cross-links are the strong hydrogen bonds between peptide chains of the tropocollagen triple helix. The intermolecular cross-links are the stable covalent cross-links between adjacent collagen molecules of the fibril. These cross-links occur at the non-helical N and C terminus of adjacent tropocollagen molecules (See Figure 1-10) [13][66]. In addition to these strong covalent bonds there are weaker non-covalent crosslink interactions between
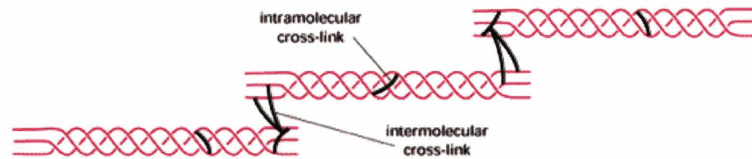
Figure 1-10: Intramolecular links are hydrogen bonds between peptide chains. Intermolecular links are convalent links between collagen molecules. These crosslinks form at the N and C terminus of the molecule [66]

fibrils which help to maintain the integrity of the structure. Many of the these non-covalent cross-links are associated with the fibril entanglement of the collagen network [7].

The intra- and intermolecular cross-links can be disrupted through an extraction process. When tissue is exposed to a given solvent, only the strong cross-links will remain intact. The weaker cross-links will be disrupted, and part of the collagen will become soluble. A measure of the soluble collagen gives a measure of the tissue's "extractability".

Danforth et al. [11] extracted human cervical tissue in a succession of water, saline, guanidine hydrochloride, and urea solutions. The study compared non-pregnant with post partum cervical tissue. A large percentage of the collagen in the post partum cervical samples were solubilized in the extractions: 84% of the original collagen of the post partum cervical tissue was extracted in the first water extraction. In the end, only 24% of the collagen in the post partum specimens remained insoluble as compared to 67% of the collagen in the non-pregnant cervix.

Kokenyesi and Woessner extracted rat cervix in 4M guanidine-hydrochloric acid solvent containing protease inhibitor. They extracted the tissue for 24 hours and separated out the resulting supernatant to analyze for collagen content. The solubility of collagen in 4M guanidine-HCl was 8 times higher at time of delivery than in the nonpregnant state. The collagen fibers were 8 times more soluble in the pregnant state because the fibers were loose and not well organized. Kokenyesi and Woessner state that this particular extraction procedure does not disrupt the covalent collagen bonds, and only disrupts the weak nonconvalent bonds (i.e. ionic and van der Waals' forces) [40].

Petersen and Uldbjerg et al. investigated the solubility of collagen in non-pregnant cervical

tissue from women with previous cervical insufficiency and women with normal obstetric history. They extracted biopsy specimens in 0.5M acetic acid containing pepsin and measured the collagen (hydroxyproline) content in the extract. The study found higher amounts of hydroxyproline in the extracts from women with previous cervical insufficiency. The extractability was 80.2% for women with previous cervical insufficiency as compared to an extractability of 49.5% for normal parous women [51]. The increased extractability in both the insufficient and post partum cervix suggests that the collagen network in the specimens is weaker than in normal non-pregnant cervical tissue. It is not known, however, if the mechanisms weakening the collagen structure in the insufficient cervix are the same mechanisms associated with cervical ripening at the time of delivery in the healthy cervix.

1.2.4   Proteoglycans and Glycosaminoglycans

Structure

Proteoglycans are glycoproteins consisting of a core protein to which at least one glycosaminoglycan chain is covalently attached [66]. They are typically identified by their glycosaminoglycan side chain. Glycosaminoglycans may also exist without the core protein as in the case of hyaluronic acid. Glycosaminoglycans are linear polymers of repeating disaccharides. Disaccharides are two linked monosaccharides which are simple sugars. The simplest GAG structure is hyaluronic acid which consists of alternating polymers of the monosaccharides N-Acetylglucosamine and glucuronic acid. Chondroitin-4 Sulfate has repeats of glucuronic acid and N-Acetylgalactosamine and is sulfated on the 4th carbon. Chondroitin-6 Sulfate is analogous to Chrondroitin-4 Sulfate but it is sulfated on the 6th carbon. Dermatan sulfate is similar to Chondroitin-4 sulfate except its repeats of L-Iduronate and N-Acetylgalactosamine [66]. Figure 1-11 illustrates the disaccharide units of common glycosaminoglycans. Each of these units is repeated to create the polymer chain of the glycosaminoglycan.

Hyaluronic acid (HA) does not link to a core protein and exists as a glycosaminoglycan in the extracellular matrix. In solution, hyaluronic acid has a randomly kinked coil structure that can entangle and form stiff networks [27]. When hydrated, pure HA can swell to one thousand times its dry weight, forming a highly viscous gel. During cervical softening hyaluronic acid concentration increases. This increase causes the tissue to imbibe water and disrupts the

(a) Hyaluron ($n \leq 50,000$)

D-Glucuronic acid · N-Acetyl-D-glucosamine

(b) Chondroitin sulfate ($n \leq 250$)

D-Glucuronic acid · N-Acetyl-D-galactosamine

Dermatan sulfate

L-Iduronic acid · N-Acetyl-D-galactosamine

(c) Heparin/Heparan sulfate ($n = 15-30$)

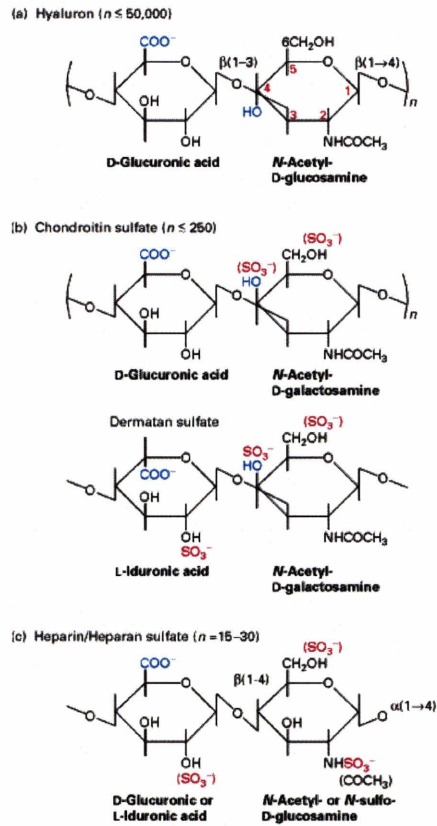D-Glucuronic or L-Iduronic acid · N-Acetyl- or N-sulfo-D-glucosamine

Figure 1-11: Glycosaminoglycans are composed of repeating dissacharides units. "n" represents the number of repeats of each unit [18].

collagen network by increasing the spacing between fibrils.

The main proteoglycan in cervical tissue is decorin, a dermatan sulfate proteoglycan. It belongs to a family of PGs called Small Leucine Rich Proteoglycans (SLRPs) which include biglycan, fibromodulin, lumican, epiphycan, and keratocan. The common feature of this family is their three domain structure. The amino-terminal domain is the attachment site for the negatively charged glycosaminoglycan. The core protein domain contains eight to ten leucine repeats. This core protein domain has a specific amino acid sequence located between repeats 4 and 6 that bind specifically to fibril types of collagen. The end domain contains two cysteine residues and its function is unknown [12]. The small leucine rich PG family is involved with regulating cell proliferation, differentiation, adhesion and migration [29].

Proteoglycans and structural glycosaminoglycans are embedded within the collagen network of the extracellular matrix. Their main function is to generate high osmotic pressure, maintaining tissue hydration and allowing the tissue to sustain compressive forces, and to regulate collagen fibril formation and spacing.

Studies of Glycosaminoglycan Concentrations During Pregnancy

An early biochemical study on human cervix was conducted by Shimizu et al. [61]. Biopsy specimens were taken from proliferative and secretory phase nonpregnant patients and from postpartum patients. Glycosaminoglycans were measured before and after specific enzymatic digestions of Streptomyces hyaluronidase, chondroitinase AC-II and chondroitinase ABC. The hyaluronic acid, chondroitin sulfate, heparan sulfate and acidic glycosaminoglycan content was higher in the post partum cervix as opposed to the nonpregnant cervix. Only the dermatan sulfate content was significantly lower in the post partum cervical specimen than in the nonpregnant specimen [61]. See Table 1.3 for glycoprotein measurements.

A study conducted by Rath et al. reports an increase in total glycosaminoglycans during pregnancy, but a large decrease in dermatan sulfate at time of parturition. Biopsy specimens were taken from 87 pregnant and nonpregnant women. Samples from the pregnant cases were taken at different stages of pregnancy: first trimester, third trimester, parturition at cervical dilation of 2-3cm, and parturition at cervical dilation of 6-8cm. It was found that the changes in proteoglycan content happens rapidly with the onset of labor. The large decrease in dermatan

Tissue	Hyaluronic Acid	Chondroitin Sulfate	Dermatan Sulfate	Heparan Sulfate	Acidic GP
Non-pregnant Proliferative	1.09 (11.6)	0.87 (9.3)	6.18 (66.0)	0.45 (4.8)	0.77 (8.2)
Non-pregnant Secretory	0.90 (10.1)	0.62 (7.0)	6.29 (70.5)	0.52 (5.8)	0.59 (6.6)
Post Partum	2.72 (17.7)	2.34 (15.2)	5.18 (33.7)	2.18 (14.2)	2.95 (19.2)

Table 1.3: Glycosaminoglycan count for human cervix from Shimuzu et al. study. Numbers are expressed in mg of GAG (in terms of hexosamine)/g dry tissue

sulfate is thought to destabilize the collagen fibers thus allowing the cervix to dilate and ripen. The results for dermatan sulfate and hyaluronic acid concentration are in Figure 1-12 [54].

Hyaluronic acid (HA) has an affinity for water molecules, thus an increase in HA concentration causes an increase in hydration for soft tissues. Maradny et al. [46] studied the HA concentration and its effects on pregnant and non-pregnant rabbit cervix. The increase in water content in the cervical tissue caused the collagen bundles to fragment and separate. The interfibrillar spaces increased and the network became less organized and less dense [46]. The study concludes that HA is responsible for increased tissue hydration, stimulation of collagenase, and ultimately control of cervical ripening. HA was injected into pregnant and non-pregnant rabbit cervix and in both cases HA induced cervical ripening and caused a large increase in water content.

1.2.5 Glycosaminoglycan and Collagen Functional Interdependence

Proteoglycans (PGs) and collagen fibers interact to maintain a balance of internal forces in the tissue and to regulate the mechanical function of the extracellular matrix. PGs induce a high osmotic pressure to imbibe interstitial water. The collagen fibers have tensile strength to counteract this swelling tendency and to limit the increase in tissue volume. The PGs also specifically bind to collagen fibrils to enhance collagen cross-linking and to regulate collagen fibril spacing. These interactions are an example of how biochemical content influence the mechanical integrity of soft tissue. Many investigators have studied the interplay between proteoglycans and collagen. Danielson et al. [12] mechanically tested skin of Decorin-null
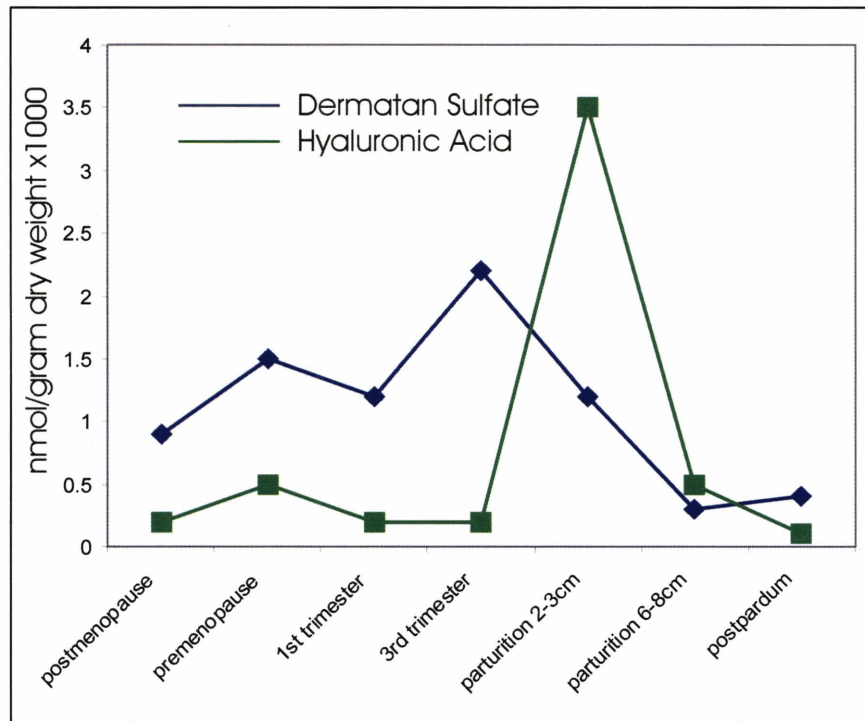
Figure 1-12: The dermatan sulfate levels in human cervix decrease significantly at parturition. The hyaluronic acid concentration increases significantly at time of parurition and falls again by time of post pardum. Graph adapted from Rath [54][18]

mice. Maroudas et al. [3] experimentally measured the osmotic pressure and tensile force in articular cartilage. Broome et al. [6] mechanically tested articular cartilage before and after proteoglycan degradation. All of these investigations noted abnormal mechanical properties when the balance between collagen and glycoproteins was disrupted.

Hydrostatic Stress Balance in Hydrated Tissue

Hydrated soft tissue maintains its shape and mechanical integrity through a balance of swelling and tensile forces. The fixed charge density associated with proteoglycans tends to imbibe fluid, and the tensile forces in the collagen network oppose the swelling tendency and limit the increase in volume. The contributing factors to the tissue swelling pressure are the Donnan osmotic interactions, the affinity between the matrix and solvent, and the thermal motion of matrix macromolecules. The Donnan electrostatic forces include the repulsive forces between charged proteoglycans and the large counterions concentration that must be present in the tissue to maintain electroneutrality. The Donnan forces decrease with increased swelling, increased bath saline concentration and decreased fixed charge density. If one component of this force balance is altered then the mechanical response of the tissue may be compromised [14].

Maroudas et al. [3] measured the collagen tensile force in articular cartilage by applying known external osmotic pressure to in-vitro human cartilage samples and measuring the resulting hydration. The external osmotic pressure was applied with calibrated baths of Polyethleneglycol (PEG) solutions, and the osmotic pressure of the proteoglycans was governed by the fixed charge density which was established by the proteoglycan concentration. The three forces considered in the Maroudas experiment were the hydrostatic stress (tensile) from the collagen network P_C, the applied isotropic pressure from the PEG bath π_{PEG}, and the osmotic pressure from the proteoglycans π_{PG}. The tensile force of the collagen network P_C and the applied isotropic osmotic pressure of the bath π_{PEG} tended to force water out of the sample. The osmotic pressure π_{PG} from the proteoglycans tended to imbibe water. The balance of forces was given by Equation 1.1.

$$P_C + \pi_{PEG} = \pi_{PG} \tag{1.1}$$

Maroudas et al. measured P_C for different cartilage samples as a function of hydration. The

samples included normal and trypsin-treated cartilage and one osteoarthritic joint. Cartilage specimens were equilibrated overnight in 0.15M NaCl. The specimen were then placed in a dialysis bag, re-equilibrated in calibrated PEG solutions, and immediately weighed to determine its hydration. The resulting osmotic pressure, π_{PG}, was then calculated from an empirical relationship between hydration, fixed charged density and osmotic pressure of a solution of isolated proteoglycans at the same concentration. The main assumption of this approach was that the osmotic pressure produced by the PGs in the tissue was equal to the osmotic pressure of isolated PGs at the same concentration. With the applied pressure π_{PEG} known, and the π_{PG} calculated from this empirical relationship, the tensile force in the collagen, P_C, could be calculated from equation 1.1. This procedure was repeated for different PEG solutions at different hydration levels.

Figure 1-13 Graph A gives an example of the balance of forces in normal adult cartilage. The collagen tensile force P_C versus hydration levels for the normal and trypsin treated cartilage samples were very similar. However, Graph B illustrates that the collagen tensile force P_C versus hydration curve for the osteoarthritic patient was much lower than the normal and trypsin treated specimens. The stiffness of the collagen network controls the level of hydration in-vivo and gave the tissue dimensional stability. The osteoarthritic samples were thought to have a weaker collagen network and therefore were unable to maintain high PG concentrations and resist mechanical loading.

In similar experiments Broom and Poole [6] enzymatically digested proteoglycans from articular cartilage and measured the compressive strength in normal and PG-free specimens. These experiments had different objectives from the studies of Maroudas et al.; Broom and Poole investigated the effects of PGs on the tissue's compressive strength, while the Maroudas study investigated the tensile strength of the collagen fibrils in osteoarthritic patients. Broom and Poole obtained articular cartilage from cows and tested three specimens from a single slice. The three specimens were incubated in three different buffer solutions: bovine testicular hyaluronidase, acetate, and Ringer's solution. The acetate and Ringer's served as the control, and hyaluronic acid was degraded and removed from the specimens subjected to hyaluronidase. Twelve specimens were tested and in each case the hyaluronidase specimens had consistently weaker compressive strengths compared to the controls. The degraded specimens lost most
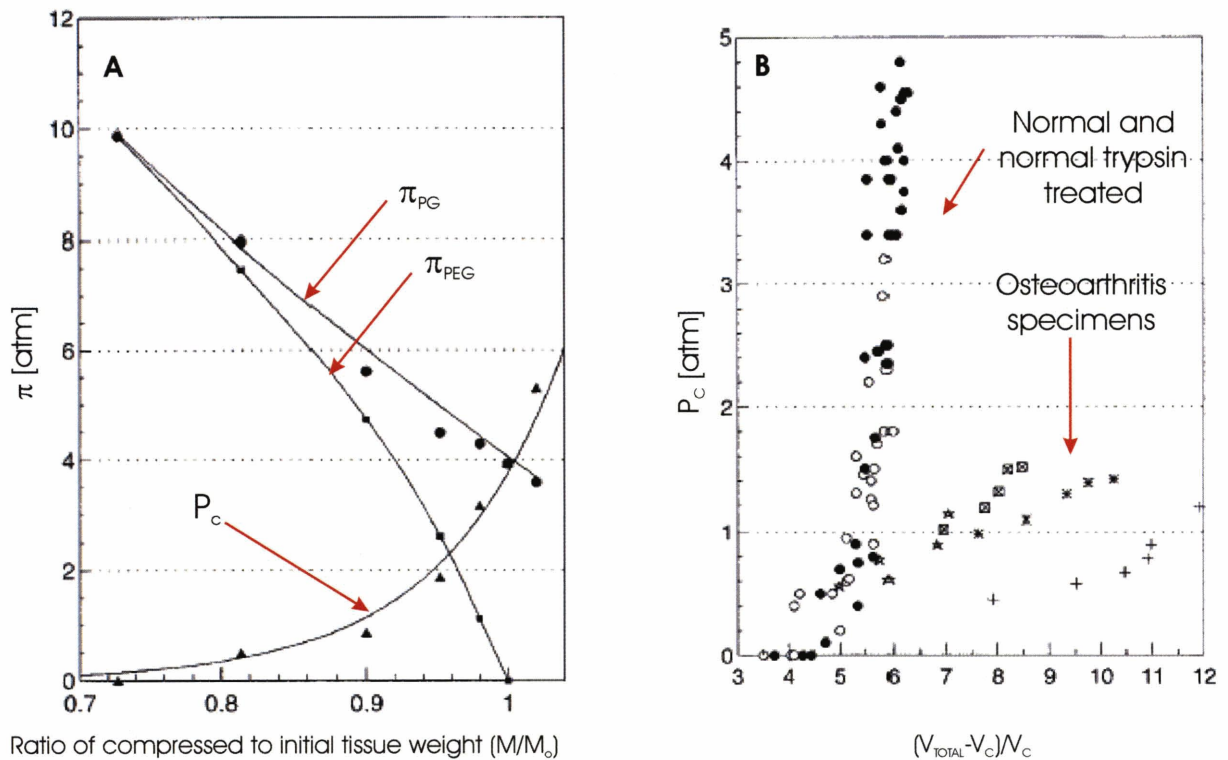
Figure 1-13: A) The forces in hydrated soft tissue in the Mardous et al. experiment are balanced between the tensile force of the collagen fibril P_c, the isotropic compressive force of the PEG solution π_{PEG}, and the osmotic pressure of the proteoglycans π_{PG}. The difference between the π_{PG} and π_{PEG} gives the force in the collagen fibril P_C. B) The collagen stiffness was considerably lower for the osteoathritus patients when compared to the normal adult cartilage samples and cartilage samples that have been treated with trypsin to rid the proteoglycans. Both graphs are adapted from Maroudas et al. [3]

of their compressive strength within one hour of incubation. Without hyaluronic acid, the collagen network became an unsupported fibrous structure and under compressive loads the collagen fibrils buckled and compacted. The control specimens in the acetate solution had a slight decrease in compressive strength when compared to the Ringer specimens, and the Ringer specimen maintained their compressive integrity during the length of all the tests.

The softening mechanisms responsible for osteoarthritis in articular cartilage is a combination of weak collagen fibrils as reported by Maroudas et al. [3] and a lower concentration of hyaluronic acid and other GAGs as reported by Broom and Poole [6]. The weak collagen fibrils allow the tissue to swell. The lack of GAGs inhibits the water binding ability of the extracellular matrix which decreases the compressive strength of the tissue. It is not fully known if these mechanisms also play a part in cervical softening or cervical insufficiency. The proteoglycans could arguably play a different role in cartilage and in cervical tissue, as the proteoglycans in cartilage have a much larger molecular weight.

Decorin-Collagen Interaction

Decorin is the main PG in healthy nonpregnant cervical tissue, representing 70% weight of all PGs. Decorin is structured to carry out specific roles in collagen network formation. Decorin binds collagen fibrils and maintains proper fibril spacing in the extracellular matrix. One collagen triple helix rod binds to the inner concave surface of the U-shape decorin. The glycosaminoglycan side chain aligns perpendicular to the collagen fibril to give correct spacing between fibrils which gives the collagen its staggered appearance. The side chain also prevents lateral fusion of collagen fibrils Figure 1-14 illustrates the relationship between decorin and a collagen fibril [25]. Keene et al. [34] confirmed that the decorin glycoprotein folds into an arch-shaped structure. This study measured the dimensions of purified decorin with rotary shadowing electron microscopy. The overall dimension were on the order of 7nm between the two arms and 5nm between the base of the arch and the apex.

Danielson et al. [12] investigated the relationship between decorin and collagen fibrillogenesis by comparing the collagen of wild mice and decorin-free, knock-out mice. The knock-out mice, compared with the wild mice controls, had extremely thin and frail skin. Immunohistochemistry results of the knock-out mice's collagen matrix showed extreme lateral fusion and
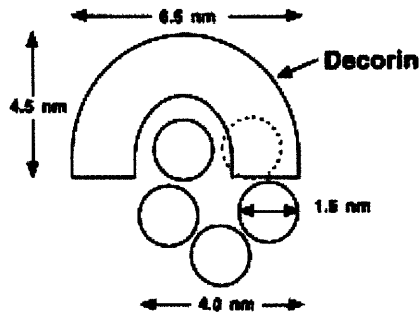
Figure 1-14: The arch-shaped decorin interacts with an individual collagen fibril. One triple helix of the fibril fits within the arch of decorin, and another triple helix interacts with the arm of decorin. Illustration from [25]

non-uniform cross-sectional profiles of collagen fibers. Collagen fibril diameters of knock-out mice ranged from 40 to 260nm whereas the collagen fibril diameters from the wild mice ranged from 40 to 180nm. Figure 1-15 shows the irregular cross-sectional profiles of collagen fibrils in the decorin-null mice. Because of the decorin deficiency, smaller fibrils fused to larger fibrils creating irregular profiles. This irregular collagen fibrils created a weak morphology and reduced the tensile strength of the skin. Figure 1-16 is the graph of the load displacement curves for the decorin-null and wild type mice. The breaking point for the wild type mice was five times higher than the one for the decorin-knockout litter. In conclusion, the Danielson team explains:

> *The evidence favoring protein-protien interaction as the major function of SLRPs*
> *is persuasive. For example, decorin binds non-covalently to the surface of the fibril-*
> *lar collagen, primarily type I, and retards the rate and degree of collagen fibrilloge-*
> *nesis in-vitro. This specific interaction is mediated by the protein core, whereas the*
> *glycosaminoglycan chain of decorin extends laterally from adjacent collagen fibrils,*
> *thereby maintaining interfibrillar spacing. This lateral orientation has also been*
> *demonstrated in collagen fibrils reconstituted in vitro in the presence of decorin.*
> *Thus, coordinated expression of decorin and associated collagens may regulate an*
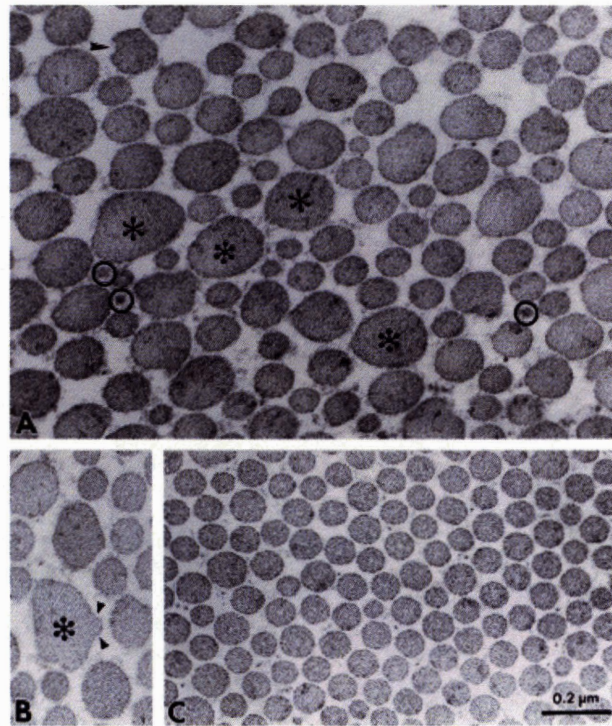> *orderly matrix assembly*[12].

Figure 1-15: A and B represent transmission electron micrographs of the dermal collagen from the decorin-null mice. C represents collagen from wild type mice. The decorin-null mice have irregular fiber diameters while the wild type mice have compact and regularly spaced fibrils [12]. ·
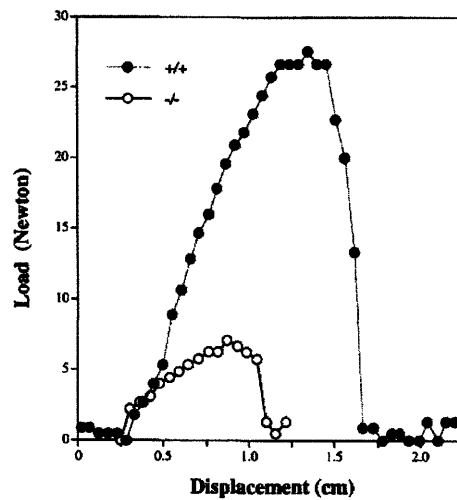
Load (Newton)

Displacement (cm)

+/+
-/-

Figure 1-16: The tensile strength of the skin from the decorin-null (-/-) mice is considerably reduced. Dumbell shaped bar specimens were made with a central cross-section $1cm^2$ The tensile specimens were pulled at a constant strain rate of 1mm/s to failure. Graph from Danielson et al. [12]

An excess of decorin, or its associated GAG dermatan sulfate, might also result in impaired tissue properties. The studies of Kokenyesi and Woessner [40] suggest that an increase in the ratio of dermatan sulfate to collagen can be responsible for cervical softening. An excess of dermatan sulfate will bind and coat a newly synthesized collagen fibril thus not allowing it to bind to other fibrils.

To investigate this hypothesis, Kokenyesi and Woessner used a rat model and measured the mechanical and biochemical properties of the cervix at different stages of pregnancy. They measured the circumference, rate of creep, and extensibility of the cervix. For the same specimens, they also measured collagen and proteoglycan concentration and the extractability of collagen in 4M guanidine-HCl. The cervical circumference was found to best correlate to cervical dilation behavior at term and post partum. Further, cervical circumference had a strong positive correlation with the dermatan sulfate to collagen ratio. As the dermatan sulfate to collagen ratio increased the cervical circumference increased. This relation was true for both softening trends at term and stiffening trends post partum.

Another finding in the Kokenyesi and Woessner study was that the total collagen content did not change significantly through pregnancy. Consequently as the total weight of the cervix

increases significantly through the gestational period, the concentration of collagen per wet weight reduces significantly during pregnancy, then rises again slightly at post partum. This finding disputes the belief that an increased enzymatic and collagenase activity causes cervical softening. Because the collagen concentration does not recover fully post partum to match the observed recovered mechanical integrity, other mechanisms must be present to stiffen the tissue. Kokenyesi and Woessner postulate that the main contribution to the recovery of tissue stiffness is the significant decrease in dermatan sulfate in the 4 hours post partum. This decrease in dermatan sulfate allows the collagen network to organize again to regain its strength.

In a similar study, Leppert and Kokenyesi [44] investigated the decorin to collagen ratio in rat gestation. They obtained cervices from pregnant rats at 5, 11, 18, and 21 days gestation. A sensitive immunohistochemical technique was used to identify the amount and location of decorin in the rat cervix. The proposed hypothesis was that: *"... decorin expression increased progressively throughout pregnancy and is consistent with the hypothesis that an excess of decorin near term is capable of initiating a decorin-collagen interaction that lead to collagen fibril disruption and decreased cervical tensile strength."* Increased decorin staining was observed with increasing gestational age. In early pregnancy, decorin was first located in the deep stroma around the stromal fibroblasts. As pregnancy continued, decorin was increasingly observed in the subepithelial stroma and in, lesser amounts, in the deep stroma. In late pregnancy, the decorin was present homogeneously throughout the cervical tissue. At this stage in late pregnancy the collagen fibers were disorganized and formed a loose network.

1.2.6 Thrombospondin 2 Deficiency

More recent work by Kokenyesi et al. [39] investigated the role of thrombospondin 2, an extracellular matrix glycoprotein, in cervical softening. The lack of thrombospondin 2 has been associated with abnormal collagen fibril morphology in skin and tendon. Kokenyesi measured the mechanical and biochemical properties of mice cervix in a thrombospondin 2 knock out line and a wild type line. Mechanical measurements included creep tests where two pins in the inner canal were pulled apart by a 50g weight. The distance between the pins were recorded with time to measure the circumference of the inner canal. Measurements were taken at a non-pregnant state, 10, 14, and 18 days gestation. Clear evidence was found that the

TSP2 knockout mice cervical tissue had altered biomechanical properties when compared to the control wild type mice.

1.3 Biochemical Assays

Literature findings reviewed in Section 1.2 illustrate the fundamental role the biochemical component of the tissue plays in its mechanical function. Biochemical tissue components can be determined by tissue-specific assays. Some common assays are reviewed in this section, including protocols for freezing and homogenizing tissue, measuring collagen and sulfated glycosaminoglycan concentration, measuring individual glycosaminoglycans, extracting and measuring weakly crosslinked collagen, estimating fixed charged density, and measuring swelling and osmotic pressure. Literature studies investigating dense fibrous tissue were reviewed, including studies on articular cartilage, cornea, skin, tendon, and cervical tissue. It was noted that the storage and handling protocols are very important to reduce enzymatic degradation of the tissue specimens.

1.3.1 Homogenization and Pulverization

Homogenization of soft tissue is attained by pulverizing and mincing the tissue sample into minute particles. Pulverization techniques require the tissue to be frozen at -80°C. If the tissue reaches room temperature the glycosaminoglycan clump together and it is very difficult to obtain an homogeneous sample. A very common method presented in the literature was to freeze the tissue with liquid nitrogen and then homogenize it in a large blender. This method works well for samples on the order of 1 or 2 grams. However, blenders are too large for smaller samples. Instead, Kokenyesi et al. ground small tissue samples with a mortar and pestle [39]. Another technique used by Hoemann et al. [30] was to smash the tissue in a biopulverizer. This device consisted of a stainless steel holder and plunger pre-cooled in liquid nitrogen. The tissue was flashed frozen in liquid nitrogen and smashed in the steel holder (See Figure 2-7 for an example of a biopulverizer).

Solvent	Yield
1. Water	Glycoproteins, Proteoglycan subunits
2. 0.5M NaCl	Collagen, Less syllable GP and PGs
3. 4M GuCl	Proteoglycan complex, Collagen
4. 7M urea, 0.2M mercapteothanol	Dislufide-linked protein aggregates

Table 1.4: Extraction method done by Danforth et al.

1.3.2 Total Collagen (Hydroxyproline) Content

Collagen concentration can be measured using a standard hydroxyproline spectrophotometric assay as described by Woessner and Stegeman[33][62]. Hydroxyproline is an amino acid unique to collagen. It exists in a 7.46 to 1 ratio with collagen[40]. To determine total collagen content, dry tissue samples are hydrolyzed to release the hydroxyproline from the peptide link. Hydrolyzation is performed by heating the tissue in 6N HCl at 110°C for 18 hours. The lowest concentration which can be detected from the assay is $1\mu g$ hydroxyproline per 2ml of solution, and the assay can be extrapolated to measure $10\mu g$ within an error of 2%.

1.3.3 Collagen Extractability

A small number of researchers have used different extraction protocols to quantify the strength of collagen bonds in cervical tissue. Danforth et al. [11] extracted pregnant and non-pregnant human tissue. Petersen et al. [51] extracted human cervical tissue with and without a history of cervical insufficiency. Kokenyesi et al. [39] extracted mice tissue with a thrombospondin 2 deficiency. Tables 1.4, 1.5, and 1.6 outline each research groups protocols. Results from these studies were discussed in Section 1.2.3.

Danforth et al. [11] gathered cervical specimens from nonpregnant and pregnant patients. The pregnant samples were obtained immediately after delivery with a biopsy punch. Care was taken to discard the mucosa and retain only the stroma portion. The tissue was frozen at -73°C until time of assay. The tissue was thawed and minced. Half of the minced tissue was dried, and the second half went through the serial extraction procedure outlined in Table 1.4. The insoluble fraction was the residue left after extraction, and the soluble fraction was the tissue dissolved in the extraction solution. The two fractions were compared to obtain extractability measurements.

37

Solvent	Method	Yield
1. 0.5M acetic acid w/pepsin	3 days at 4C	Extractable Collagen

Table 1.5: Extraction method of Petersen et al.

Solvent	Method	Yield
1. Tris Buffered Saline	30 min. at 4°C	non-crosslinked collagen
2. 1M NaCl	24 hours at 4°C	non-crosslinked collagen
3. 0.5M Acetic Acid	24 hours at 4°C	acid-labile, aldimine-crosslinked collagen
4. 1% SDS and 5% β-mercaptoethanol	boil 15 min.	heat-labile keto-amine-crosslinked collagen, collagen associated proteins

Table 1.6: Extraction method of Kokenyesi et al.

Petersen et al. [51] performed a single extraction step with 0.5M acetic acid containing pepsin (1mg/ml). Biopsy samples were obtained from nonpregnant women with previously diagnosed cervical insufficiency and women with a normal obstetric history. Each sample was dried, cut into small pieces, and defatted. The minced pieces were extracted for 3 days at 4°C in the 0.5M acetic acid solution. The supernatant and residue pellet were assayed for hydroxyproline concentration. The extractability was defined as the hydroxyproline concentration in the supernatant divided by the total hydroxyproline concentration.

Kokenyesi et al. [39] studied thrombospondin 2-null (TSP2-null) mice to understand its role in cervical softening. Samples were taken at different stages of pregnancy from normal and from TSP2-null mice. The complete cervix was excised, frozen in liquid nitrogen, and ground. The powdered tissue was submitted to a series of extractions outlined in Table 1.6. Each extraction solvent also contained a cocktail of proteinase inhibitors consisting of 10mM EDTA, 1mM PMSF, 10mM N-ethylmaleidmide, and 5μg pepstatin. The supernatants obtained from extraction steps 2 and 3 were further dialyzed against 3 changes of Tris/HCl. The supernatants from each extraction was assayed for hydroxyproline content. The amount of hydroxyproline in the supernatant compared to the total amount was the measure of extractability.

1.3.4 Proteoglycans and Glycosaminoglycans

A widely accepted spectrophotometric assay for measuring sulfated glycosaminoglycans in tissue is the dimethylmethylene blue (DMB) assay. The standard reference for this assay is Farndale et al. [17].

Shimizu et al. measured glycosaminoglycan concentration in non-pregnant and post partum human cervix. To homogenize the samples, 10g of wet weight was excised from the cervix. The sample was cut into small pieces and homogenized in a Waring blender with 30mL of 80% ethanol. The homogenate was heated for 3 minutes at 100°C and the suspension was centrifuged. The sediment was washed twice with ethanol and once with ether. The samples were then dried to a constant weight. To estimate crude glycosaminoglycan content, 2g of dry sample were digested twice with 80mg of pronase P and GAG content was measured with an Alcian Blue technique.

Plaas et al. identified and quantified specific glycosaminoglycan disaccharides in cornea and cartilage using a Fluorophore-Assisted Carbohydrate Electrophoresis (FACE) technique [52][53]. Tissue samples were digested with enzymes specific to the disaccharide. Chondroitinase ABC cleaved chondroitin and dermatan sulfate, and hyaluronidase cleaved hyaluronic acid. Each disaccharide product produced a free reducing end which was tagged with a fluorescent marker. The tagged products were resolved by electrophoresis using high concentration polyacrylamide gel, and the disaccharides were identified by their characteristic migration. Under an ultraviolet light, the fluorescent tag gave a stoichiometric signal for each reducing end of the disaccharide product. The molar fluorescence was estimated by measuring the average pixel density per picomole of the standards and comparing it to the samples. Images were recorded and analyzed with computer imaging software.

1.4 Mechanical Characteristics of Cervical Tissue

The existing literature on the mechanical characteristics of cervical tissue is very limited. Past experiments have been restricted to uniaxial testing, and past models for the tissue have been restricted to one-dimensional linear elasticity or viscoelasticity. Harkness and Harkness [24] performed the earliest mechanical tests on pregnant and non-pregnant rat cervix specimens. They tested specimens at different stages of gestation, and measured the elongation of the cervix under tension at a constant 50g load. They applied the load by inserting two steel rods along the inner canal, and measured the elongation by measuring the distance between the rods. The modulus of elasticity was calculated as the fractional change in breaking tension

Inner OS	Middle	Outer OS
65.59±6.59 MPa	42.13±4.26 MPa	24.69±3.38 MPa

Table 1.7: Stretch Modulus of longitudinal sites along the cervix. Sites closer to the inner os have a higher mechanical resistence.

over the fractional change length. In non-pregnant cervix tissue the modulus of elasticity was found to be $3\text{x}10^9$ dynes/cm^2 (300MPa) and in pregnant cervix (21 days gestation) the modulus of elasticity was $1\text{x}10^9$ dynes/cm^2 (100MPa). It was noted that non-pregnant cervix tissue typically reached an equilibrium elongation under constant load. However, the pregnant cervix specimens continued to elongate until final rupture [24].

Early studies on human cervix from hysterectomy specimens were conducted by Conrad et al. [9]. Uniaxial tension tests were performed on pregnant and non-pregnant specimens obtained from different radial and longitudinal locations along the cervix. The tension specimens were sutured to fixtures and pulled at a rate of 0.1cm/min. Figure 1-17 illustrates the drastic difference in the mechanical properties of pregnant and nonpregnant cervix specimens where the non-pregnant cervix was significantly stiffer than the pregnant cervix. Also, the non-linear stiffening behavior present in the non-pregnant cervix was absent in the case of the pregnant specimen, which continued to elongate. To identify the location of highest mechanical resistance of the cervix, Conrad et al. excised tension specimens at different locations along the length of the cervix, as well as radially from the inner canal. The study found that the site of maximum resistance was at the inner os within a 5mm thick annulus of stroma immediately adjacent to the inner canal. Table 1.7 gives the stretch modulus at specific longitudinal positions. Figure 1-18 illustrates the difference in mechanical stiffness for specimens located at different radial positions from the inner canal [9].

Stys et al. [63] measured the compliance of cervical tissue using an ewe model. The study established that cervical softening was independent from uterine contractions, and that the biochemical remodelling of the tissue was responsible for cervical softening. Measurements were taken on three groups of ewes: a control group, a group with induced labor with uterine contractions, and a group with induced labor without uterine contractions. The team continually measured intrauterine and cervical pressure while infusing water at a constant rate into a donut-shaped cervical balloon. The compliance was measured as the change in volume over the
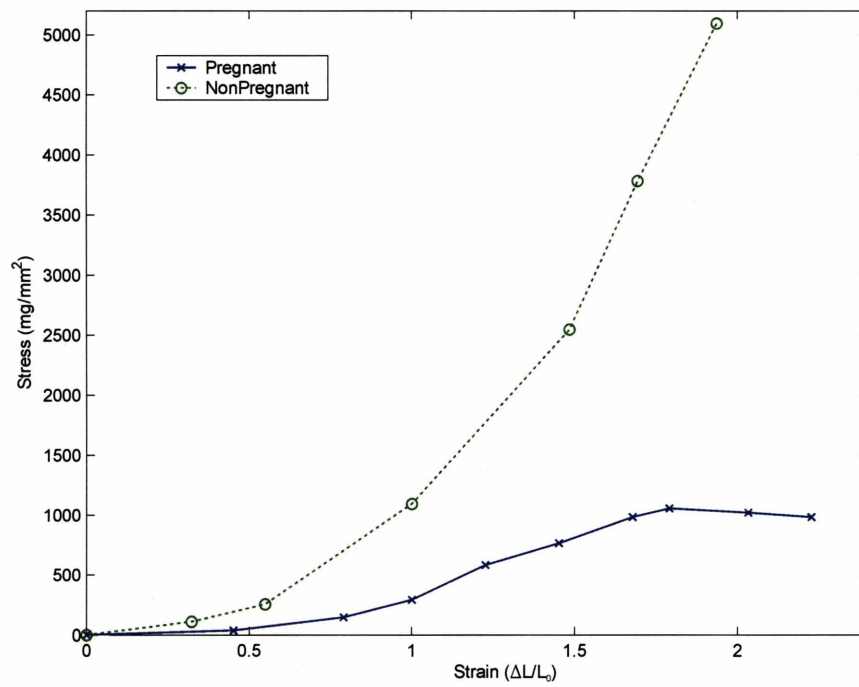
Figure 1-17: Stress strain curves of pregnant and non-pregnant cervix from the Conrad uni-axial tension experiments.
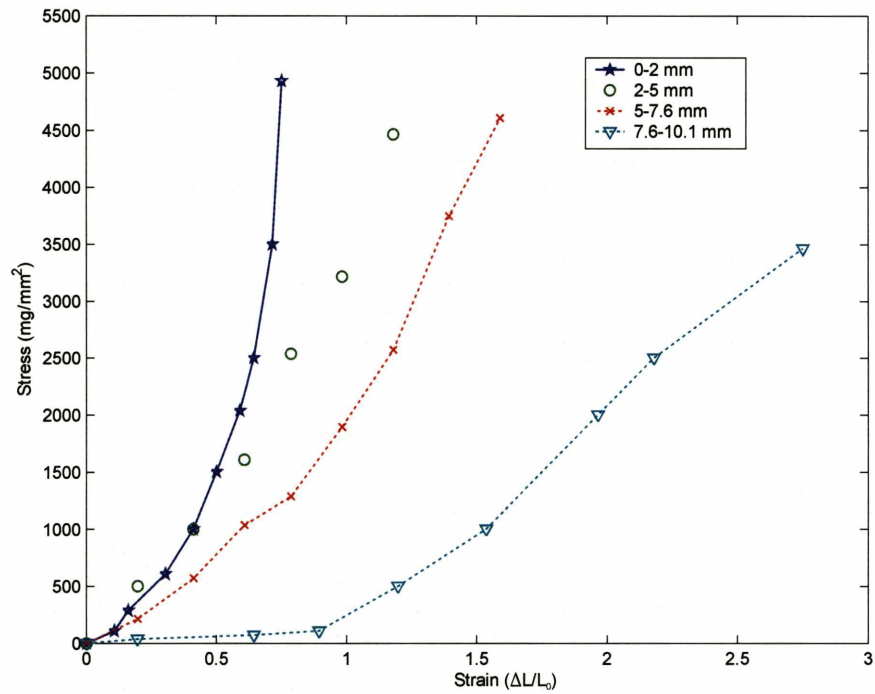
Figure 1-18: Stress strain curves adapted from Conrad's data for non-pregnant cervix in uniaxial tension. The location of specimens were measured from the inner canal. Tissue samples become stiffer as they become closer to the inner canal.

Group	3cm balloon elastance	4cm balloon elastance	number of patients
Experimental - previous preterm birth	90mmHg/ml	61mmHg/ml	247
Control - no previous preterm birth	130mmHg/ml	95mmHg/ml	42

Table 1.8: Mean elastance of non-pregnant cervix in patients with previous preterm birth and no previous preterm birth from the Kiwi et al. study.

change in pressure. It was found that the cervix softens regardless of the presence of uterine contractions.

A more recent study on human cervical tissue by Kiwi et al. [36] used a balloon method to measure cervical elastance. The mean elastance was defined as the change in pressure over the change in volume. The study was conducted on a group of women with a history of previous preterm birth and on a control group. Preterm birth was defined as women who had previously had one or more spontaneous midterm pregnancy losses or three or more early spontaneous abortions. Results of this study are in Table 1.8. In this study, 3 or 4 cm balloons were inflated in the cervical canal of nonpregnant women and the mean cervical elastance was measured. A significant difference between the experimental and control groups was noted. There was also a large spread of elastance between patient to patient. The range of differences between control subjects is on the order of 300mmHg/ml. Obstetrical history was recorded for both groups to see if historical risk factors had an affect on the elastance. A two-way analysis of variance was performed on both sets of balloon data and it was found that parity of the patient strongly affected the elastance data. It was concluded that the traditional methods for diagnosing cervical insufficiency should accompany a more objective method such as balloon elastance measurement.

Chapter 2

Methods

The mechanical and biochemical experimental methods in use at the time of this publication are reported below. Concise procedures are in Appendix A. The experimental protocols attempt to prevent enzymatic degradation and to reduce variability while conducting in-vitro tests on cervical tissue samples.

2.1   Tissue harvesting and specimen preparation

Hysterectomy specimens from pre-menopausal women with benign gynecological conditions were obtained from the Tufts - New England Medical Center. One cervix was obtained from a pregnant patient who had undergone two prior cesarean deliveries. She was diagnosed with placenta increta and underwent an elective cesarean hysterectomy at 34 weeks. Non-pregnant cervices were categorized according to parity and labeled NPND for women with no previous vaginal deliveries and NPPD for women with previous vaginal deliveries. The pregnant specimen was labeled PCS (Table 2.1 summarizes the obstetric cases tested). Approval from the Institutional Review Board was obtained from both Tufts - New England Medical Center and MIT prior to initiating the study.

The uterus and cervix were excised from the patients and placed on ice. A custom designed stainless steel sectioning tool (Fig. 2-1) was used to obtain from each cervix four 4mm parallel disks perpendicular to the inner canal. The slicing device contains custom surgical blades from Speciality Blades Inc, and the engineering prints are in Appendix B.

Obstetric History	Abbreviation
Non-Pregnant: No Previous Vaginal Deliveries	NPND
Non-Pregnant: Previous Vaginal Deliveries	NPPD
Pregnant: Taken at time of Cesarean Section	PCS

Table 2.1: Three obsetric cases studied.

Each cervical slice was labeled to distinguish position relative to the internal and external os (Fig. 2-1). The cervical tissue slices were stored flat at -80°C (Fig. 2-2). Preliminary tests performed on fresh and previously frozen tissue from the same cervical slice confirmed that freezing does not alter mechanical properties, a result consistent with similar findings for cartilage (see, e.g. [35]).

Prior to testing, each 4mm slice was thawed for approximately 3 minutes in phosphate buffered saline (PBS) at an ionic concentration of 0.15M. Mechanical and biochemical specimens were cut exclusively from the cervical stroma. The location of the cervical stroma in relation to the cervical mucosa is illustrated in 2-1. For compressive mechanical tests, cylindrical specimens were cut with an 8mm biopsy punch at the same radial location for each slice. Care was taken in labeling the samples according to their anatomical site because data in the literature [9] indicate some variation in mechanical properties with longitudinal position along the axis of the cervix, and radial distance from the cervical canal. For biochemical specimens, approximately 20mg of tissue adjacent to the location of the mechanical specimens were excised from the stroma. Each cervical slice yielded compression specimens (1 to 3 specimens, depending on the visual homogeneity of individual slices) and several biochemical specimens. The mechanical specimens were weighed and equilibrated overnight in PBS at 4°C, and the biochemical specimens were stored at -80°C until time of pulverization.
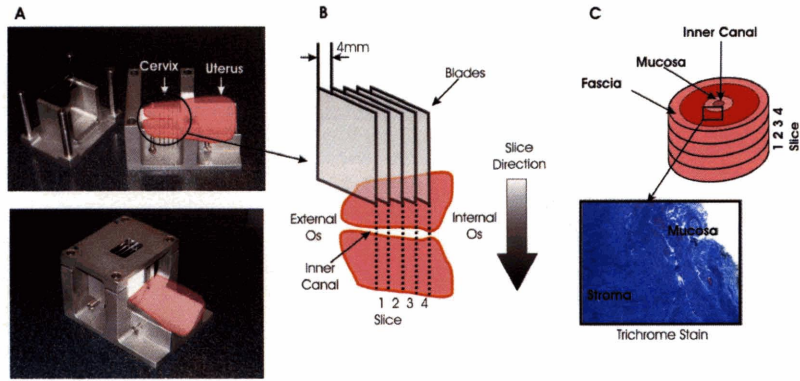
Figure 2-1: Specimen preparation. A) Stainless steel sectioning tool. B) Cervical slice labeling convention and blade orientation. C) Cervical tissue. The mucosa is the soft cellular layer lining the cervical canal. The stroma is the firm fibrous inner core

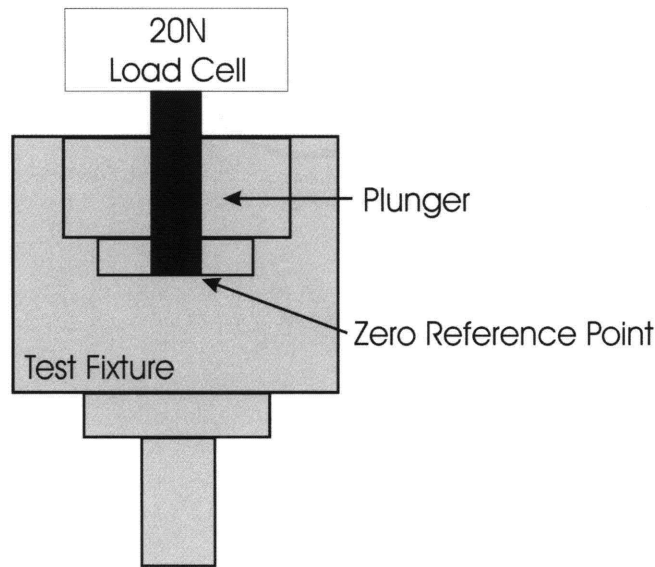Figure 2-2: Plastic device used to store cervical slices.

Figure 2-3: Reference location during mechanical tests

2.2 Mechanical Experiments

2.2.1 Setup

All tests were conducted on a universal material testing machine (Zwick Z2.5/TS1S, Ulm, Germany) with the specimens immersed in a PBS bath in custom-designed acrylic fixtures (Fig. 2-4, engineering drawings in Appendix B). A 20N load cell was used to collect compression data, and a 500N load cell was used to collect tension data. Video extensometer data was collected with a Qimaging Retiga 1300 CCD camera equipped with a 200mm f/4 Nikon lens. Strain data was obtained with Digital Image Correlation (DIC) techniques using the Correlated Solutions VIC-2D (version 4.4.0) software. All mechanical specimens were equilibrated overnight in PBS at 4°C, weighed, and measured prior to testing. A discussion of the motivation and implications for this equilibration procedure, which alters the hydration level of the tissue, is presented in Chapter 4.

The plunger was referenced to zero before each day of mechanical testing. The reference position was the bottom of the fixture well. See Figure 2-3 for reference diagram. To set the reference, the plunger was slowly lowered until a load differential of 0.25N is sensed by the load cell.
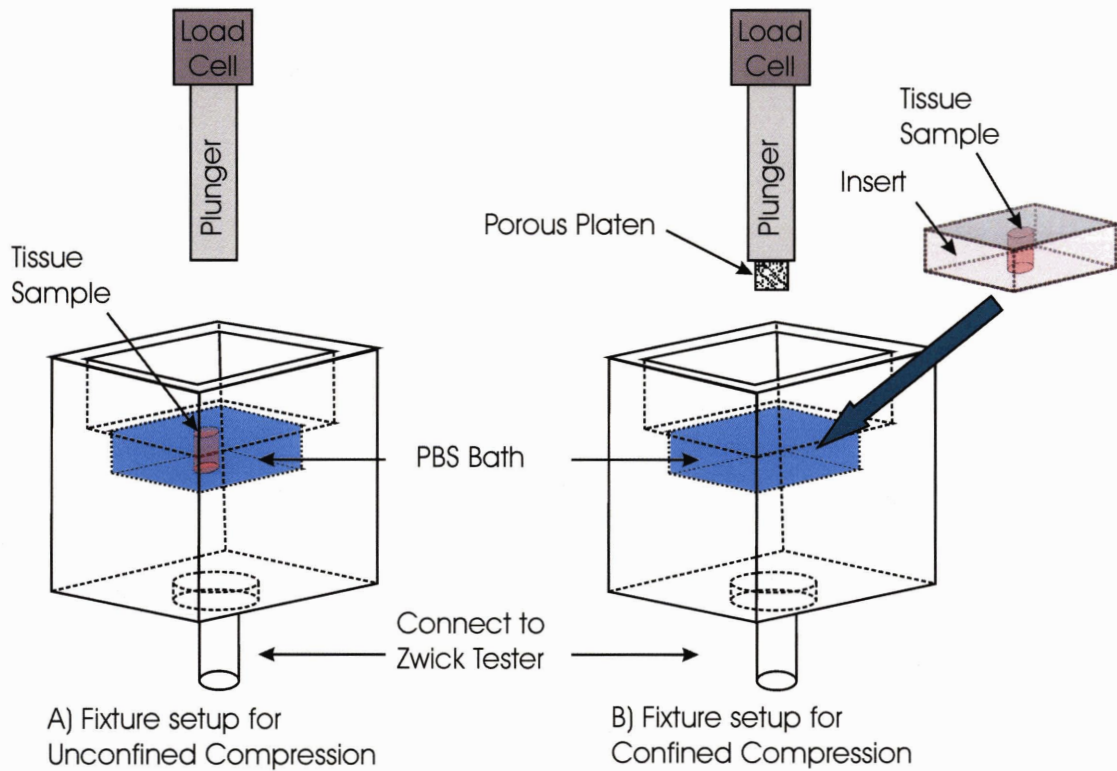
Figure 2-4: A) Setup for unconfined compression. B) Setup for confined compression. The tissue sample is placed in an insert then placed in the bath.

2.2.2 Testing

Each compression specimen was subjected to three different testing modes: load-unload cycle; unconfined ramp-relaxation; and confined ramp-relaxation. A preload of 0.005N (corresponding to a compressive stress of 100 Pa on a 8mm diameter specimen) was imposed on each sample prior to testing in order to accurately determine the sample thickness and, for the confined compression tests, improve confinement.

Fig. 2-5 illustrates the imposed deformation histories for the three tests. The compression testing protocol for each specimen consisted of the following sequence of tests: (1) load-unload

cycle, (2) unconfined ramp-relaxation, (3) load-unload cycle, (4) confined ramp-relaxation. Each specimen was first loaded in unconfined compression to 15% axial-engineering strain and unloaded to 0% strain at a constant engineering strain rate of 0.1% s^{-1}. This load-unload cycle was repeated three times. After re-equilibration in an unloaded state for at least thirty minutes in PBS at 4°C, the specimen was subsequently subjected to an unconfined ramp-relaxation test to axial-engineering strain levels of 10%, 20%, and 30% with a ramp strain rate of 0.17%s^{-1}. Each strain level was held for 30 minutes to measure the relaxation response of the tissue. After re-equilibration in an unloaded state for at least thirty minutes in PBS at 4°C, the load-unload cycle test was repeated. The measured response was compared to the response recorded in the first load-unload test to verify that the specimen had not undergone any degradation altering its mechanical response. The specimen was then allowed to re-equilibrate for 30 minutes in PBS. After equilibration, the specimen was placed in an 8mm impermeable rigid well and subjected to a confined ramp-relaxation test to axial strain levels of 5%, 10%, and 15% with a ramp strain rate of 0.017%s^{-1}. Each strain level was held for 30 minutes to measure the relaxation response of the tissue. The history of radial stretch for the unconfined compression tests (both load-unload cycles and ramp-relaxation) was recorded using the video extensometer. The video capture frequencies for the load-unload cycle and the ramp-relaxation test were 2 Hz and 0.2 Hz respectively. Figure 2-5 shows a typical video image for an unconfined compression test.

True Stress Calculations

Force, axial displacement, and time data were collected with the Zwick Test Control software (Version 10.1). Video images with their respective time, force, and load information were collected with the Correlated Solutions Vic-Snap software. The true stress for the unconfined ramp relaxation and load-unload cycle tests were calculated based on the specimen's current area. The current area was determined from the specimen width measured with the Vic-2D extensometer.

The Vic-2D extensometer tracked the radial displacement of the cervical specimen based on a reference image taken at time of the preload. Figure 2-6 depicts the software interface for Vic-2D. Extensometer points were chosen midway between top and bottom of the sample. The pixel location of these points were tracked throughout the deformed images. No bending
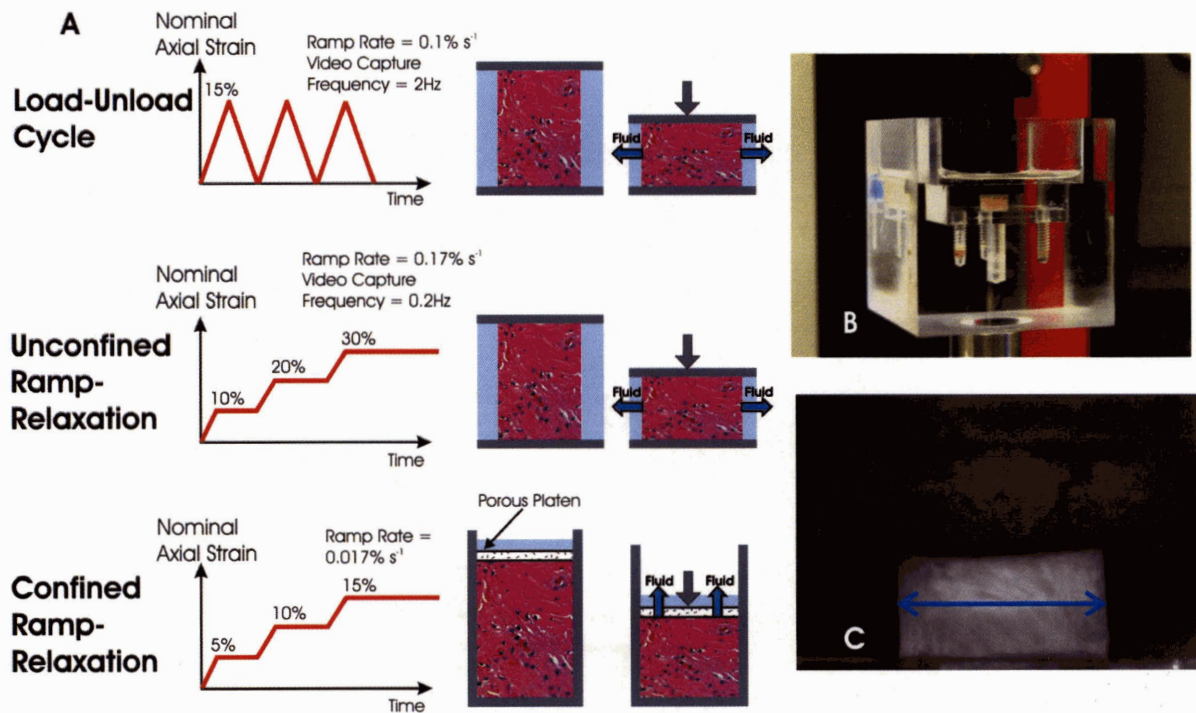
49

Figure 2-5: Compression test protocol. A) Imposed deformation history for each testing mode. B) Cervical specimen in compression fixture. C) Cervical specimen in unconfined compression. Radial stretch history is recorded by a video extensometer.

or buckling of the sample was observed. The pixel locations for each deformed image were recorded with the corresponding time, displacement, and force data from the material tested.

2.3   Biochemical Experiments

Cervical tissue samples for the three (NPND, NPPD and PCS) clinical cases were subjected to biochemical analysis. Biochemical assays measured cervical tissue hydration, collagen content, collagen extractability, and sulfated glycosaminoglycan content. Cervical tissue was defatted and homogenized prior to all biochemical assays.

Homogenization

The cervical tissue was homogenized and pulverized before all biochemical tests. To pulverize the tissue, approximately 20mg of wet tissue was wrapped in aluminum foil and flash frozen in liquid nitrogen. A biopulverizer chamber (Figure 2-7) was also pre-cooled in liquid nitrogen for approximately ten minutes. The frozen tissue was then crushed within the pre-cooled chamber using a hammer. The flattened tissue was then placed into pre-weighed 1.5mL eppendorf centrifuge tubes. The tubes were re-weighed to calculate the tissue wet tissue weight. The samples were stored at -80°C until time of biochemical assay. Care was taken not to let the tissue thaw before assay.

Hydration

The tissue hydration was calculated from the wet and dry weights of the cervical tissue. Sample weights were taken in pre-weighed 1.5mL eppendorf tubes on a micro balance. Wet weight was measured after pulverization, and dry weight was measured after 24 hours of freeze drying. Hydration was calculated using Equation 2.1.

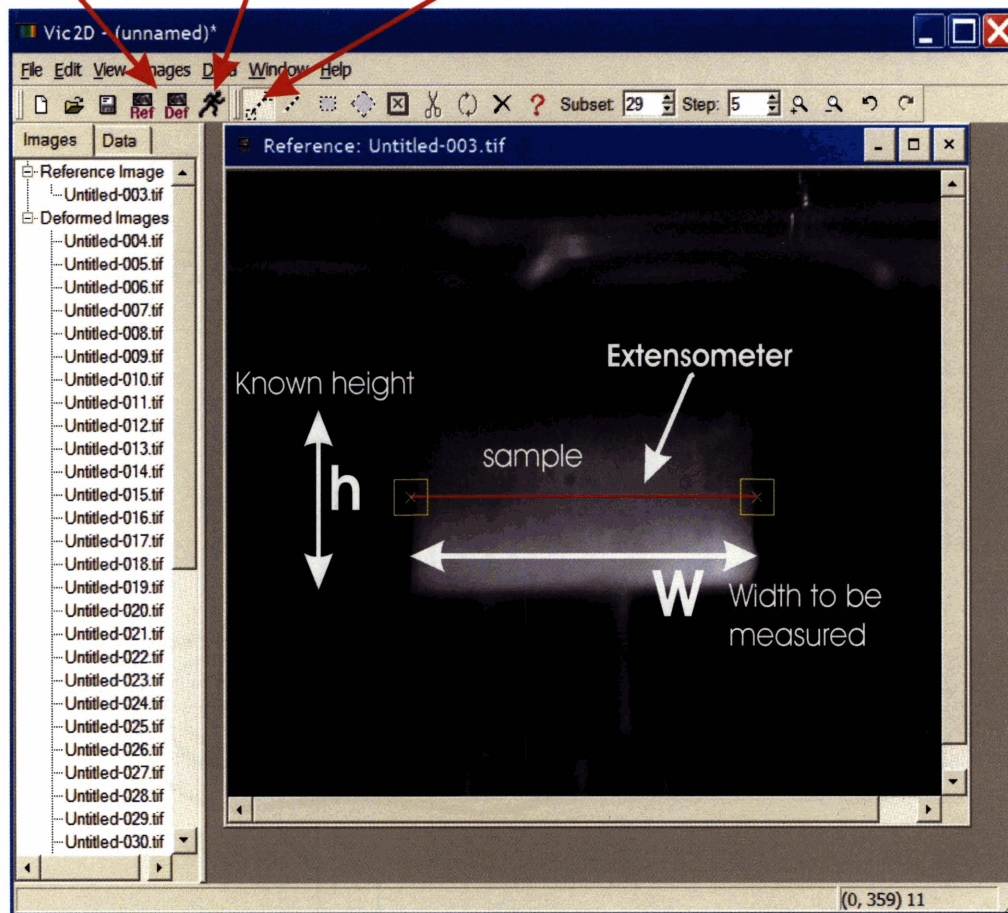$$hydration = \frac{\text{wet weight - dry weight}}{\text{wet weight}} \tag{2.1}$$

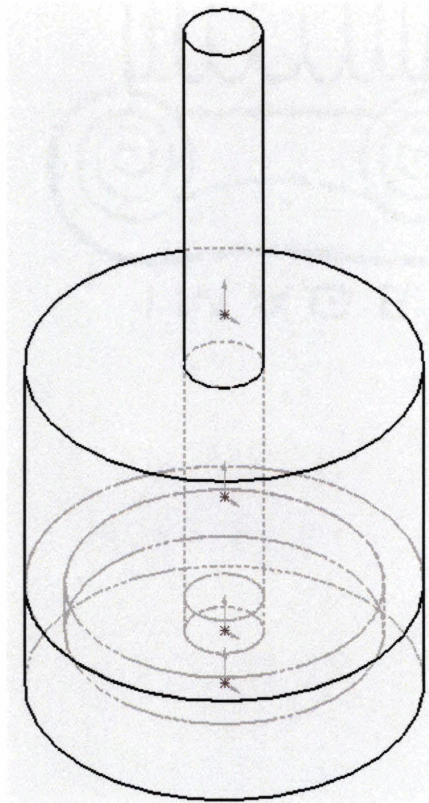Figure 2-6: Steps 1-3 to run the extensometer tool in the Vic-2D software (Version 10.1).

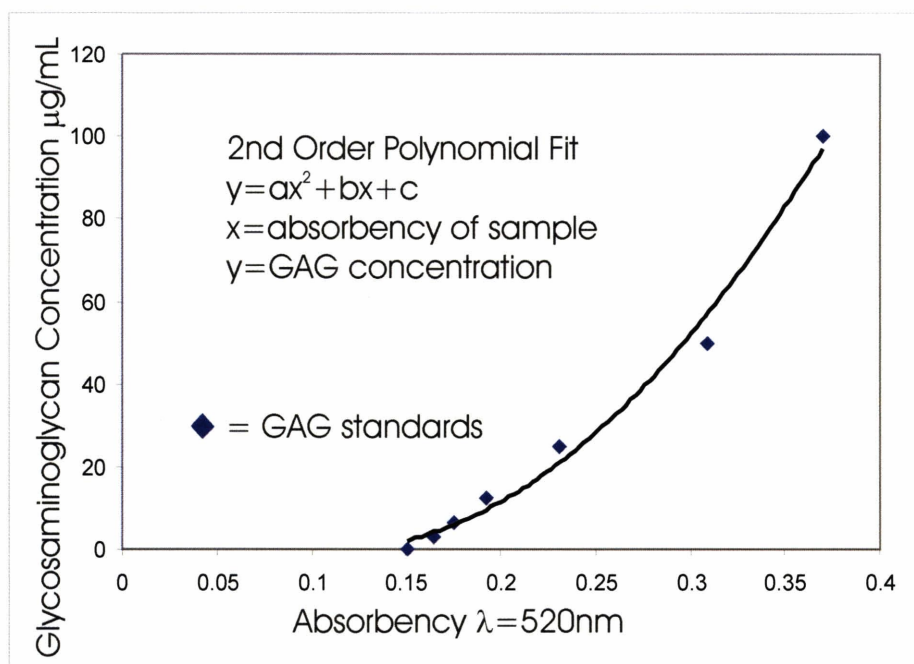Figure 2-7: The biopulverizer chamber to homogenize cervical tissue

Figure 2-8: A 2nd order polymomial used to fit the standard data points.

Sulfated Glycosaminoglycan - Dimethylmethylene Blue (DMB) Assay

Sulfated glycosaminoglycans (GAGs) content was measured using a standard DMB (Dimethyl-methylene Blue) assay [17] with chondroitin-6-sulfate (Sigma-Aldrich) as the standard. Approximately 20mg of wet cervical tissue was pulverized and then freeze-dried overnight. The dry tissue was then incubated overnight in 1mL of 0.1mg/mL solution of proteinase K (Roche Applied Science). After incubation, the tissue was assayed for sulfated GAGs using a 1,9-Dimethylmethylene blue dye (Polyscience INC). A spectrophotometer measured the absorbency of the samples at a wavelength of 520nm. A calibration curve was derived from the chondroitin-6 sulfate standards (e.g. Figure 2-8). All calibration curves were a 2nd order polynomial fit to the standard data points. The GAG concentration in terms of the tissue dry weight was calculated by Equation 2.2. See Appendix A for protocol.

$$\text{Gag concentration} = \frac{\text{GAG concentration measured [mg/ml]}}{\text{dry weight concentration loaded into well [mg/ml]}} \qquad (2.2)$$

Collagen Concentration - Hydroxyproline Assay

Collagen content was measured following a standard hydroxyproline assay referenced in Woessner [33] and Stegemann and Stalder [62]. The hydroxyproline content was obtained using a colorimetric procedure, and was converted into collagen content using a mass ratio of collagen to hydroxyproline of 7.64:1. Collagen content was normalized by tissue dry weight.

This hydroxyproline protocol was a variation of a procedure used for articular cartilage. Cervical tissue samples were pulverized and then freeze dried for 24 hours. Dry samples were transferred to preweighed 11mL Pyrex tubes and weighed for tissue dry weight. After weighing, 1mL of 6M HCl was added to the sample tube and vortexed. The Pyrex test tubes were sealed with rubber Teflon caps and the heated at 115°C overnight for hydrolyzation. After hydrolyzation, the samples were titrated using HCl and NaOH. Deionized water was used to bring each of the sample tubes to the same volume (11mL). Sample concentration before the assay dilution was calculated by Equation 2.3.

$$\text{sample concentration before dilution} = \frac{\text{dry weight (mg)}}{11\text{mL}} \tag{2.3}$$

Hydroxyproline (Sigma-Aldrich) standards of known concentrations were assayed along with the tissue samples. The samples and standards were mixed with Chloramine T for 20 minutes and p-Dimethylaminobenzaldehyde (pDAB) for 30 minutes at 60°C. After these reactions, the absorbancy of the samples and standards were read with a spectrophotometer microassay at wavelength of 560nm.

A linear regression line for the measured absorbancy versus known hydroxyproline concentration was used as a calibration curve for the samples. Figure 2-9 plots a typical calibration curve. The collagen concentration per dry weight of tissue was calculated by dividing the measured collagen concentration by the sample concentration loaded into the well. Equation 2.4 calculates the collagen concentration per dry weight of cervical tissue.

$$\frac{\text{collagen concentration}}{\text{dry weight of cervical tissue}} = \frac{\text{collagen concentration measured in microwell } \left(\frac{mg}{mL}\right)}{0.1 \cdot \frac{\text{dry weight } (mg)}{11(mL)}} \tag{2.4}$$
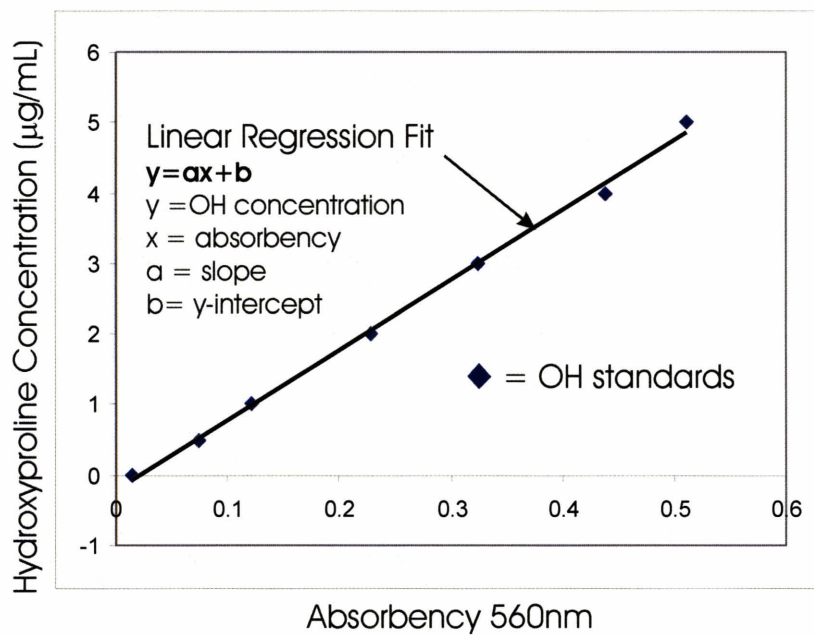
Figure 2-9: The calibration curve for the known hydroxyproline (OH) standards is a linear regression fit of the standard's data points. The above graph is an example of data points collected from the standard concentrations.

Collagen Extractability

Collagen extractability was measured by extracting approximately 20mg of wet pulverized tissue in 0.5M acetic acid containing 1mg/mL of pepsin (150μL/mg wet tissue) for 3 days at 4°C. The sample was centrifuged at 15,000g for 1 hour and the supernatant and tissue pellet were stored at -80°C. The hydroxyproline content was measured in the tissue pellet and the supernatant. The extractability is defined as the fraction of hydroxyproline in the supernatant compared to the total amount of hydroxyproline.

Chapter 3

Results

Mechanical and biochemical properties were measured for NPPD, NPND, and PCS clinical cases. The appearance and the texture of cervical tissue were visibly different for the three clinical cases. The pregnant tissue was noticeably softer and the collagen network appeared to be loosely connected, in agreement with observations reported in the literature [43]. The non-pregnant tissue appeared fibrous, with a densely connected collagen network, especially for the NPND clinical cases.

The cervical tissue was mechanically characterized by three different modes of deformation. Tests measured the loading and unloading behavior in compression. Mechanical tests also measured the stress relaxation response in unconfined and confined compression at ramp strain steps up to 30% and 15%, respectively. Results were averaged among cervices with the same obstetric history, and on average non-pregnant cervix was stiffer than pregnant cervix at peak and equilibrium stresses. Also, NPND cervices were stiffer than NPPD cervices when investigating the averaged data. However, the statistical power of this study was not strong enough to report a statistical difference.

Biochemical assays measured cervical tissue hydration, collagen content, collagen extractability, and sulfated glycosaminoglycan content for the three obstetric cases. On average, pregnant cervix had a higher hydration and collagen extractability when compared to non-pregnant tissue. No difference was detected in the collagen content and the sulfated glycosaminoglycan content between pregnant and non-pregnant specimens.

3.1 Mechanical Characterization

While substantial variations in the amplitude of the stress response for different cervical tissue specimens were apparent, the qualitative features of the tissue response were remarkably consistent. In view of this observation, rather than focusing on individual test results, data is presented in terms of the averaged response for each of the three considered clinical cases. Several individual test results are also presented in the Discussion section, where specific issues relating to the selected testing protocols and experimental findings are discussed. Although the number of specimens tested for each clinical case was too low to yield a sufficient statistical power, the trends in recorded averages for all modes of testing are consistent with clinical observations and data in the literature: PCS specimens displayed substantially reduced amplitudes in their stress response, and NPND specimens displayed the highest stress amplitudes for all modes of deformation.

Compression tests were performed on 9 specimens from the three NPPD cervices, 3 specimens from the two NPND cervices, and 2 specimens from the PCS cervix. Figure 3-1 shows the averaged stress responses of the tissue to the load-unload compression cycles for the three clinical cases. The material displays a nonlinear response, with marked hysteresis. The first loading cycle is consistently associated with a stiffer response and more substantial hysteresis. While the unloading response is not substantially altered between cycles, the response in subsequent loading ramps becomes slightly more compliant, so that the amount of hysteresis is reduced. Differences between the first and second cycles are less pronounced than the difference between the second and third cycles. This softening behavior with subsequent deformation cycles has been observed in other classes of soft tissues and it is often referred to as "conditioning". Standard variations in peak stress (at 15% axial strain) for the three obstetric histories are reported in Table 3.1. The averaged peak stresses in Figure 3-1 indicate an order of magnitude difference between the averaged responses for the NPND and PCS cases.

Figure 3-2 shows the averaged stress responses of the tissue to the ramp-relaxation tests in unconfined and confined compression for the three clinical cases. For both modes of deformation, the first compression ramp is associated with a relatively low peak stress. The second ramp and third ramps are associated with higher peak stresses, increasing nonlinearly with applied axial strain. The relaxation behavior is probably associated with at least two separate mechanisms.
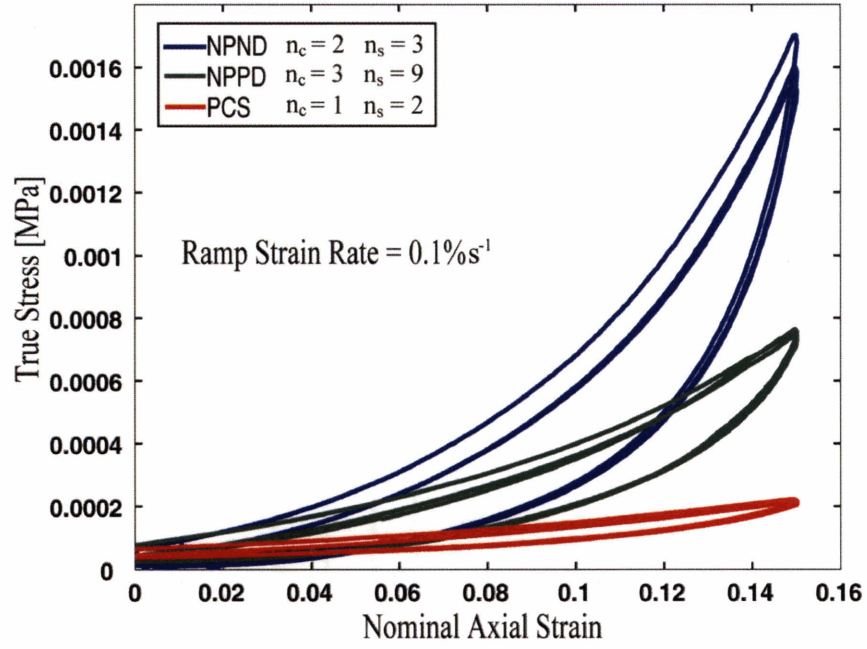
Figure 3-1: Cervical stroma response to uniaxial compression cycles. The initial cycle is the highest loop in each set, and subsequent cycles are associated with lower peak stress levels. Experimental curves were averaged for each obstetric case.

Obstetric Case	n_c	n_s	Standard variation in peak stress
NPND	2	3	± 0.0028MPa
NPPD	3	9	± 0.0008MPa
PCS	1	2	± 0.0001MPa

Table 3.1: Standard variation in peak stress values (at 15% axial strain) for the load-unload compression tests

Substantial relaxation occurs in a very short time interval (~10s) following the end of the loading ramp. Stress relaxation continues then at much lower rates, so that a relaxed state is only partially attained at the end of the 30-minute relaxation interval. Although the unconfined compression test subjects the specimens to two-fold levels of axial strain, and a ten-fold ramp strain rate, as compared to the confined compression tests, the recorded peak stresses and equilibrium stresses are comparable for the two testing modes. Also, relaxation times appear to be slightly reduced for the unconfined compression cases. These observations can be partially explained in terms of differences associated with the diffusion of interstitial fluid, which plays a major role in the transient response of the tissue. In the unconfined compression configuration, the specimen surface in contact with the bathing solution is essentially doubled (sample radius and thickness are approximately equal), which allows for faster outflow of the interstitial fluid. Furthermore, the confined compression configuration imposes a volumetric strain on the tissue equal to the axial strain, while in the unconfined compression configuration the specimen is free to expand radially (friction effects between specimen and compression platens are negligible). In the unconfined compression configuration the volumetric strains (and thus interstitial fluid outflow) are therefore controlled by the balance between the bulk and shear stiffness of the specimen.

Averaged radial stretch histories for the three clinical cases in unconfined ramp-relaxation tests are reported in Figure 3-3. For purely isochoric deformation, compressive axial strain of 10%, 20% and 30% would correspond to radial stretches of 1.05, 1.11,and 1.20, respectively. Comparing these values with the curves in Figure 3-3, we see that the specimens undergo a substantial volume change in unconfined compression tests. The radial stretch histories indicate that these volume changes (and therefore the outflow of interstitial fluid) are more significant for the NPPD and PCS cases.

For both deformation modes, PCS specimens displayed substantially reduced amplitudes in their stress response, and NPND specimens displayed the highest stress amplitudes. Figure 3-4 and Figure 3-5 show the (pseudo-)equilibrium and peak stresses for unconfined and confined compression, respectively. Standard variations in peak stresses and equilibrium stresses are reported in Table 3.2. For both unconfined and confined compression tests, and for all three clinical cases, the increase in equilibrium stresses with axial strain was nearly linear, while
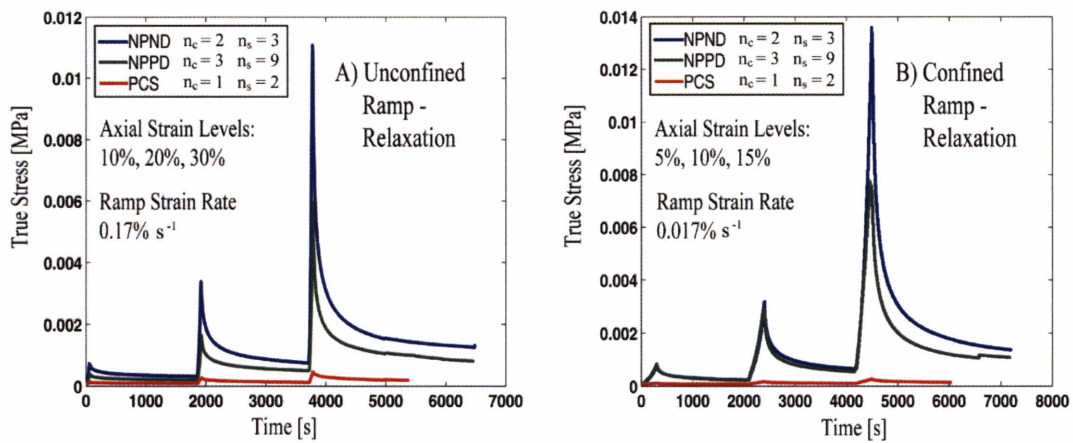
Figure 3-2: Cervical stroma response to ramp-relaxation in (A) unconfined compression, and (B) confined compression. Experimental curves were averaged for each obstetric case
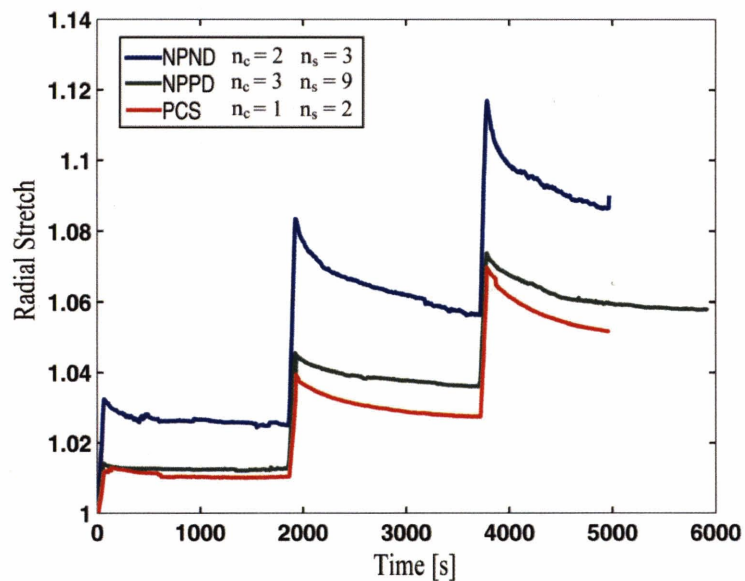

Figure 3-3: Radial stretch of specimens subjected to ramp-relaxation unconfined compression. Experimental curves were averaged for each obstetric case
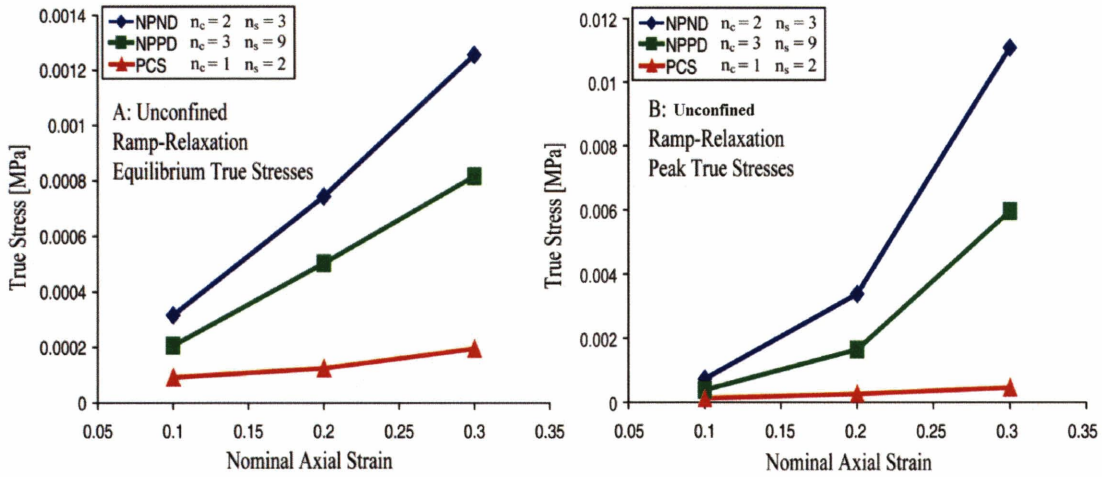
Figure 3-4: Averaged stress levels for the three obstetric cases in unconfined ramp-relaxation compression tests. (A) Equilibrium stresses and (B) peak stresses measured at axial strain levels of 10%, 20%, and 30%

Obstetric Case	n_c	n_s	Unconfined Equilibrium	Unconfined Peak	Confined Equilibrium	Confined Peak
NPND	2	3	±0.0015MPa	±0.0156MPa	±0.0014MPa	±0.0143MPa
Non-Pregnant:	3	9	±0.0006MPa	±0.0096MPa	±0.0012MPa	±0.0125MPa
Pregnant:	1	2	±0.0001MPa	±0.0001MPa	±0.0001MPa	±0.0001MPa

Table 3.2: Standard variation in stress levels for ramp-relaxation compression tests

the increase in peak stress was nonlinear. While the peak stress levels for the non-pregnant specimens were an order of magnitude higher than the equilibrium levels, the peak stress levels for the pregnant specimens were not substantially higher than the equilibrium levels. Since fluid diffusion controls the transient peak response, this result is consistent with qualitative observations of the tissue morphology: much higher hydraulic permeability coefficients are probably associated with the loosely connected pregnant tissue.

3.2 Biochemical Analysis

Cervical tissue samples for the three (NPND, NPPD and PCS) clinical cases were subjected to biochemical analysis. Biochemical assays measured cervical tissue hydration, collagen content,
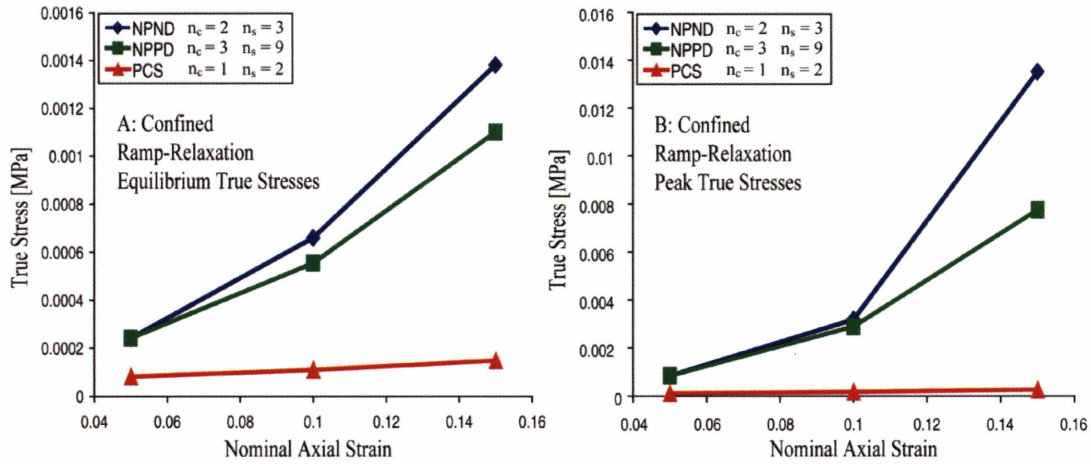
63

Figure 3-5: Averaged stress levels for the three obstetric cases in confined ramp-relaxation compression tests. (A) Equilibrium stresses and (B) peak stresses measured at axial levels of 5%, 10%, and 15%

collagen extractability, and sulfated glycosaminoglycan content. Table 3.3 reports the biochemical content measured for the three clinical cases. Data was averaged among cervices with the same obstetric history. Table 3.3 gives both average values and standard deviations over the number of samples (n_s) analyzed for each assay.

A significant ($p<0.05$) difference in hydration was established between pregnant and non-pregnant specimens. Differences in collagen extractability were in agreement with trends reported in the literature [11][61]. Extractability levels increased twofold from NPND tissue to NPPD tissue, and again increased twofold from NPPD tissue to PCS tissue, where 86% of the collagen was extractable in 0.5M acetic acid with pepsin. Due to the low trial numbers of the extraction experiments, a statistically significant difference cannot be strictly established. No statistically significant difference in collagen content between non-pregnant and pregnant clinical cases could be determined. Sulfated glycosaminoglycans content was not measured in the pregnant tissue and differences in sulfated glycosaminoglycans content between the two non-pregnant cases were not significant.

64

Obstetric History	Hydration (% per dry weight)	Collagen Content	Collagen Extractability	Sulfated GAGs (% per dry weight)
NPND	77.6±2.2% n_s=17	65.45±5.4% n_s=3	26.3±6.4% n_s=3	1.06±0.65% n_s=10
NPPD	79.3±2.0% n_s=51	74.9±8.9% n_s=11	44.0±7% n_s=2	1.17±0.56% n_s=14
PCS	87.2±1.6% n_s=3	79.5±11.1% n_s=2	86.6±1.2% n_s=1	N/A

Table 3.3: Results of biochemical assays

Chapter 4

Discussion and Conclusions

Currently, diagnostic tools for identifying cervical insufficiency are limited because the underlying biochemical and mechanical mechanisms remain elusive. It is known that a combination of anatomical, biochemical, mechanical, and obstetric factors are attributed to the cause of cervical insufficiency. However, these factors taken alone cannot predict the outcome of pregnancy. It is the interrelationship of these factors which can determine the course of pregnancy.

This study had two complementary objectives: first, the establishment of a stringent experimental protocol to collect data on the biochemical composition and to collect mechanical properties of cervical tissue under different loading modes; second, a preliminary investigation of normal ranges of variation in tissue properties among both non-pregnant and pregnant patients. In order to validate our specimen handling and mechanical testing protocols, we investigated the repeatability of property measurements for "equivalent samples". Equivalent samples are specimens obtained from the same anatomical site (same longitudinal and radial position) from a single patient. We found that to obtain repeatable results, a number of precautions were necessary, including the storage of cervical slices at -80°C at time of excision until time of experiments to prevent tissue degradation, and the equilibration of mechanical specimens overnight in PBS at 4°C prior to testing. Here we provide a discussion of the motivation and implications of our testing protocols, and offer further details on the collected experimental data.

4.1 Lessons Learned from Preliminary Mechanical and Biochemical Tests

The current mechanical and biochemical experiments have evolved from protocols gathered from the literature and colleagues. Preliminary experimental trials determined parameter changes to the original protocols. Mechanical test parameters include specimen size, tissue composition, thawing rate, equilibration behavior, bathing solution, loading patterns, and handling technique. Biochemical assay parameters include pulverization technique, weighing technique, tissue digestion, and extraction solution. In the discussion which follows in this section, lessons learned from preliminary experiments are presented and results are given to support current experimental procedures.

4.1.1 Mechanical Characterization

Specimen Size

Uniform specimen size and shape was important for mechanical test repeatability and reliability. Early data from Febvay's thesis in Figure 4-1 illustrated large stress response variabilities from specimen to specimen [18]. Inconsistent tissue handling and preparation were responsible for the variations. Before the use of the stainless steel slicer (Figure 2-1 on Page 46), cervical slices were cut with a surgical scalpel after soaking in saline at room temperature. Samples prepared with these methods were not uniform because the scalpel did not ensure even 4mm slices and the saline-soaked slices were uneven. Because of the non-uniform test specimens, mechanical data was unreliable. In response to these inconsistencies, the stainless steel slicer was developed to cut the cervix into even 4mm slices, and the cervical slices were immediately frozen after cutting to maintain their shape.

A variety of biopsy punch diameters (6mm, 7mm, and 8mm) were tested to determine which diameter cored the best cervical specimen. The 8mm punch produced the most uniform specimens. The 6mm diameter punch was too small compared to the height of the sample; The larger aspect ratio caused the samples to become skewed. The 7mm punch was a dedicated stainless steel Keyes biopsy punch, and the blades were dull and required much maintenance
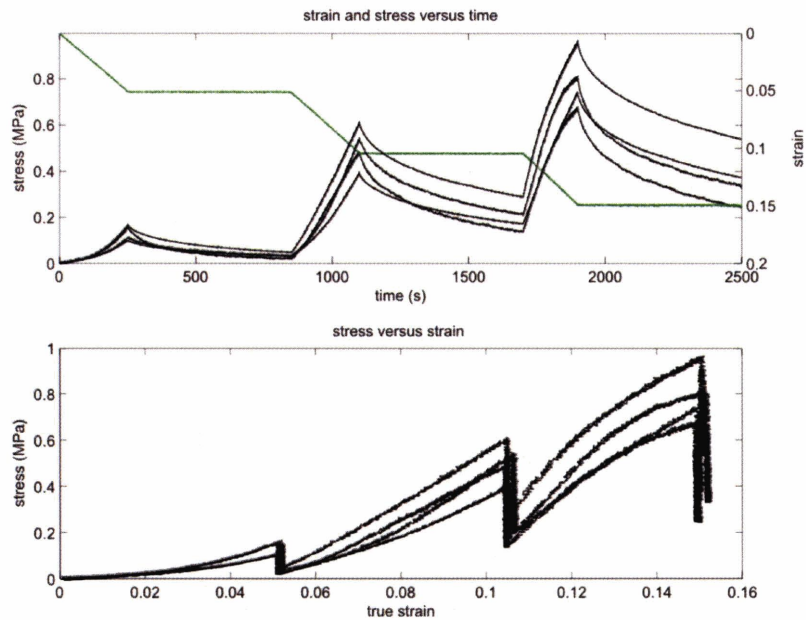
Figure 4-1: Mechanical test results from Febvay thesis. Consistent tissue handling protocols were not used to ensure specimen homogeneity and to prevent tissue degradation [18].

Freezing and Thawing

Freezing the tissue specimens did not alter its mechanical properties. Investigators, including Maroudas, Oyen and Kiefer, noted that freezing does not alter mechanical properties of soft tissues [3][50][35]. Freezing the tissue directly after surgery was beneficial because it preserved the tissue biochemistry and it maintained the tissue shape after slicing.

The accuracy of the cylindrical shape of the specimen obtained with the punch was dependent on how long the cervical slice was allowed to thaw after it was taken out of the freezer and before the specimen was cored. Figure 4-2 illustrates the stress response in confined ramp-relaxation compression of three nonuniform samples taken from a single cervical slice from a NPPD cervix. The specimens were loaded to strain steps of 5, 10, and 15% at a ramp rate of 1% per minute. The cervical slice thawed for 20 minutes in a PBS bath before specimens were cored from the stroma The resulting specimens and their stress responses were inconsistent because the cervical slice had heterogeneously swollen. It was observed that thawing the specimen for 3 minutes and then coring the stroma produced the most uniform test specimens.
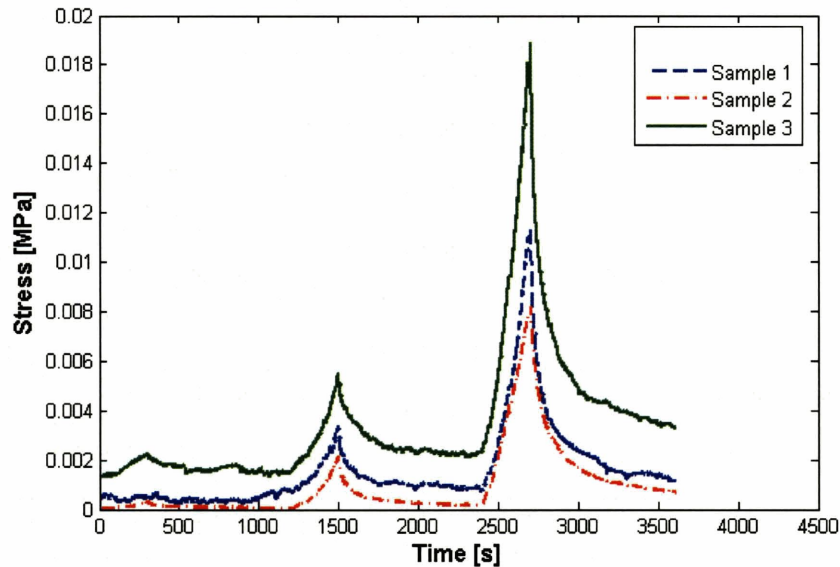
68

Figure 4-2: Stress response in confined compression for three samples from a cervical slice from a NPPD cervix. Samples were loaded to 5, 10, 15% strain steps at a rate of 1%/minutes. The cervical slice thawed for 20 minutes before stroma samples were cored.

Swelling and Equilibration

An important aspect of the proposed protocols is tissue equilibration. The hydration levels of the stroma significantly affect its mechanical response. As mechanical specimens are excised from the surrounding tissue, constraints from the interconnected collagen network are relaxed. When the excised tissue is placed in saline at physiological concentration, the specimen will then swell to reach a new equilibrium state at a higher hydration level. Typical swelling curves for compression specimens are shown in Figure 4-3A where the wet weights of two specimens are plotted as a function of the hydration time in PBS. These curves display a rapid rise in hydration level, immediately following the placement of the specimen in saline, with exponentially decreasing hydration rates over time. Typical characteristic time constants for this hydration transient (~5hr) are unfortunately comparable with testing time intervals. If a specimen is not allowed to properly equilibrate prior to testing, the testing results will be confounded by the superposition of effects due to the hydration process.

Figure 4-3 illustrates the engineering stress-strain response in unconfined compression for

69

two samples which were allowed to fully equilibriate. Sample 1 was tested at 6.5, 8, and 24 hours of equilibration, and Sample 2 was tested at 7.5, 9, and 24 hours of equilibration. There was small variabilities between the load-unload response of the tissue at the different equilibration times. The stress response was similar because after 6.5 hours both tissue samples were fully equilibrated with their surrounding bathing solution. Soaking the tissue overnight at 4°C does not alter tissue properties.

Figure 4-4 demonstrates the significant influence of hydration levels on the measured mechanical properties. Two compression samples were excised from the same cervical slice and tested after short hydration intervals (1.5 and 3 hrs). The sample that was allowed to hydrate for a longer interval displayed a stiffer response. The same specimens were then placed in saline, equilibrated overnight and retested. A noticeably stiffer response was obtained for the fully equilibrated specimens. Interestingly, the sample that had appeared stiffer proved to be the more compliant of the two when equilibrated. The argument could be put forward that the adopted equilibration protocol alters the tissue properties from their in-vivo state. However, the purpose of this investigation was not to obtain absolute values of tissue properties, but rather to identify overall qualitative features of the tissue response, and to investigate relative variations in properties between specimens from patients with different obstetric histories. The equilibration protocol is evenly applied to all samples, and the increased hydration level only affects the amplitude of the stress response and not the qualitative feature of the curves. For the purpose of this investigation, the effects of the equilibration step are therefore inconsequential. In future studies, we propose to use a stronger ionic bath, both in the equilibration and in the mechanical testing procedures, to limit the swelling of the tissue and reach equilibrium hydration levels comparable to the in-vivo levels.

Inhomogeneous Tissue Samples

The mechanical properties of the cervical specimens were highly dependent on the tissue composition. Figure 2-1 on Page 46 illustrates the different tissue layers of the cervix. The stroma is the tough fibrous inner core, and the mucosa and fascia are the soft cellular outer layers. Mechanical testing proved that inhomogeneous specimens containing mucosa and fascia do not give a representative estimate of the tissue strength.
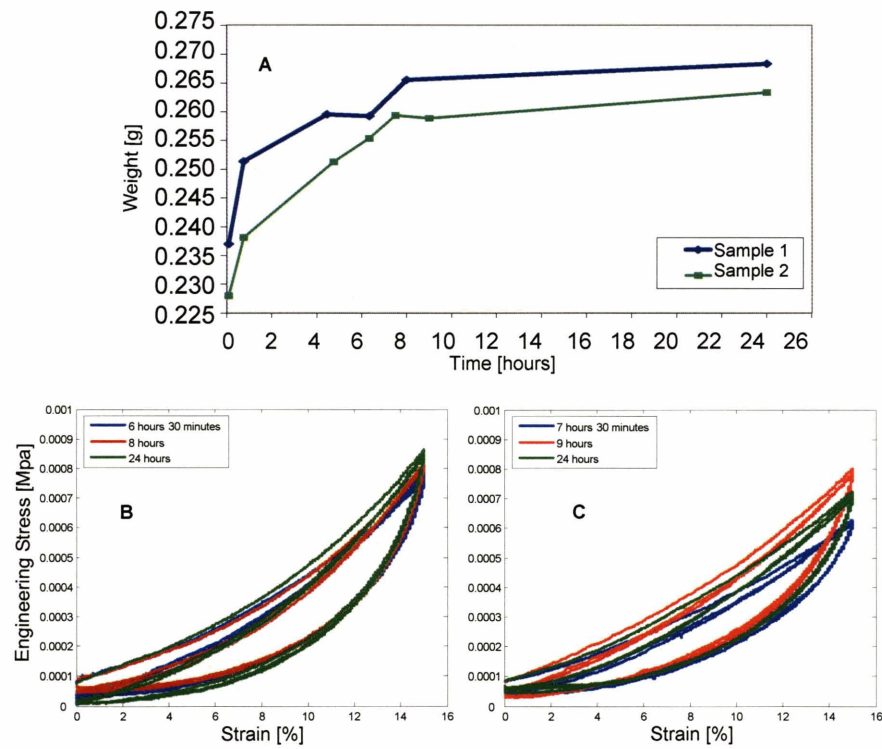
Figure 4-3: A) Swelling curve from two compression specimens obtained from the same cervical slice B) Stress-strain behavior of Sample 1. C) Stress-strain behavior of Sample 2.
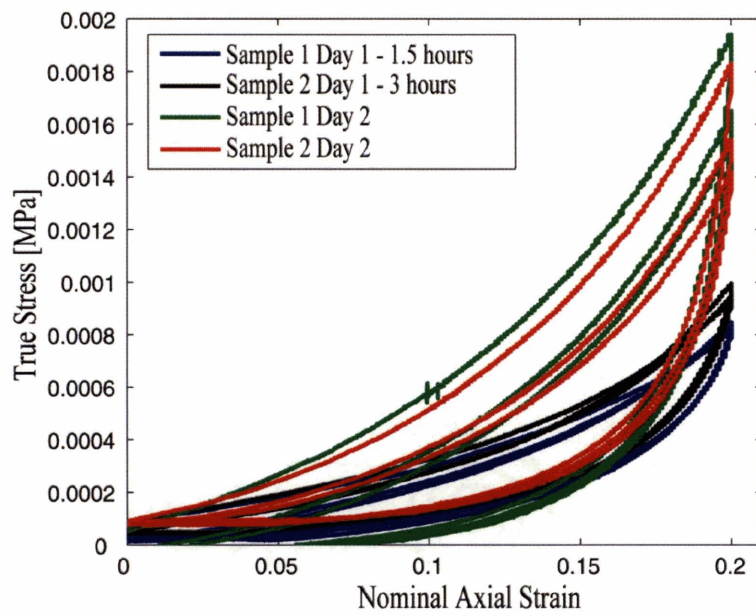
Figure 4-4: Stress response of two samples from the same cervical slice taken from a NPPD cervix. Samples were tested shortly after cutting and then again after 24 hours of equilibration. The samples had a stiffer response after 24 hours of equilibration.
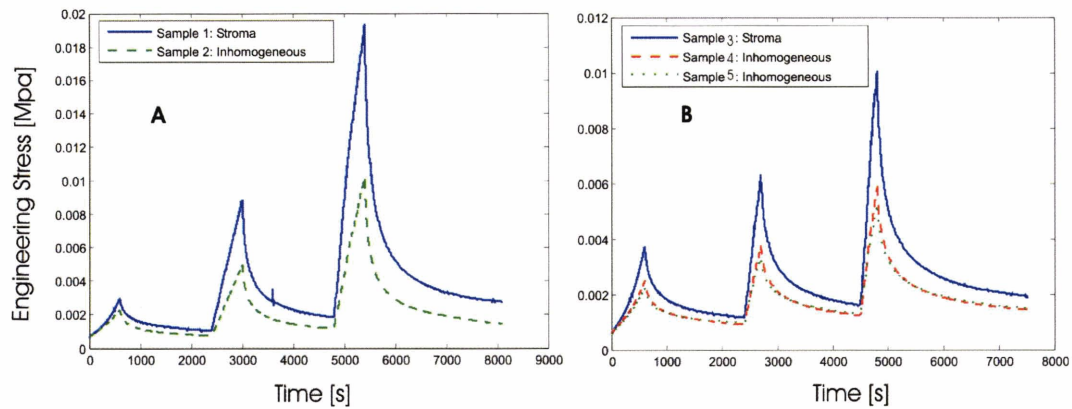
Figure 4-5: Unconfined compression data from A) Samples from cervical Slice 3. B) Samples from cervical Slice 4 of a NPPD cervix. Inhomogeneous tissue samples had a lower mechanical strength than homogeneous stroma samples.

Figure 4-5 illustrates the unconfined ramp-relaxation response of homogeneous and inhomogeneous samples. Samples 1 and 3 had a homogeneous stromal tissue consistency, and samples 2, 4, and 5 were inhomogeneous with a combination of stroma, fascia and mucosa. Samples were tested in unconfined compression at strain levels of 10%, 20%, and 30% and at a ramp rate of 1% per minute. The preload was 0.025N, and the bathing solution was a combination of saline and protease inhibitors.

The homogeneous tissue samples were stiffer in unconfined compression. The inhomogeneous samples had a lower peak and equilibrium stress response because the mucosa does not have load bearing properties.

Bathing Fluid

The proper bathing fluid was important for mechanical experiments because the ionic properties of the fluid effected the swelling and equilibrium properties of the tissue. Two bathing solutions were tested: phosphate buffered saline (PBS) and a solution with salt and protease inhibitor. It was found that PBS preserved the tissue throughout testing, while the protease inhibitor cocktail (containing 0.15M NaCl, 10mM EDTA, 1mM PMSF, 10mM N-ethylmaleimide, and 5μg pepstatin) did not preserve the tissue during mechanical tests. The pH of the protease inhibitor solution was too low, and the increased acidity altered the mechanical properties of

the tissue because it disrupted the equilibrium of the charged particles within the tissue.

Mechanical tests were done on four samples from cervical slice 1 of a NPPD cervix. Two samples were tested in 0.15M NaCl solution and two sample were tested in the saline protease inhibitor cocktail. The 0.15M NaCl solution had the same pH and salt molarity as PBS and therefore considered equivalent. Each sample was tested twice in a load-unload cycle in unconfined compression to 15% strain after 24 hours of equilibration. Figure 4-6 illustrates the engineering stress-strain behavior of the four samples.

The specimens tested in saline had better repeatability when compared to specimens tested in the protease inhibitor solution. The two specimens tested in the protease inhibitors had a large variability between load-unload tests.

Testing the Same Tissue Sample

The testing protocols in Chapter 2 allowed us to obtain consistent mechanical response for tests on "equivalent samples", i.e., samples obtained from the same anatomical site from a single cervical specimen. Variations in the measured response between "equivalent samples" are very limited (see Figure 4-7A) as long as care is exercised in obtaining homogeneous specimens of neat stroma. In agreement with the findings of Conrad et al. [9], we noted some degree of variability in stroma properties for samples excised from the same cervix but at different anatomical sites (see Figure 4-7B). Differences between the response of the tissue for the same cervix at different longitudinal positions (i.e., different tissue slices) can be comparable to differences between the response of specimens obtained from different patients (Figure 4-7C). In general, however, we noted larger variability in tissue properties between patients (even patients with the same obstetric history) than between specimens from the same cervix. The standard variation in the stress levels reported in Tables 3.1 and 3.2 is due to the combined effects of averaging specimen responses from different patients and from different cervical anatomical sites.

The experimental protocol outlined in Chapter 1 was designed to provide sufficient data to uniquely determine the constitutive material parameters that describe the mechanical behavior of the tissue. The complex compression-testing program allowed us to quantify the effects of different deformation modes and deformation rates on the response of each tissue sample. However, we found that the compression tests alone were insufficient to provide all the data
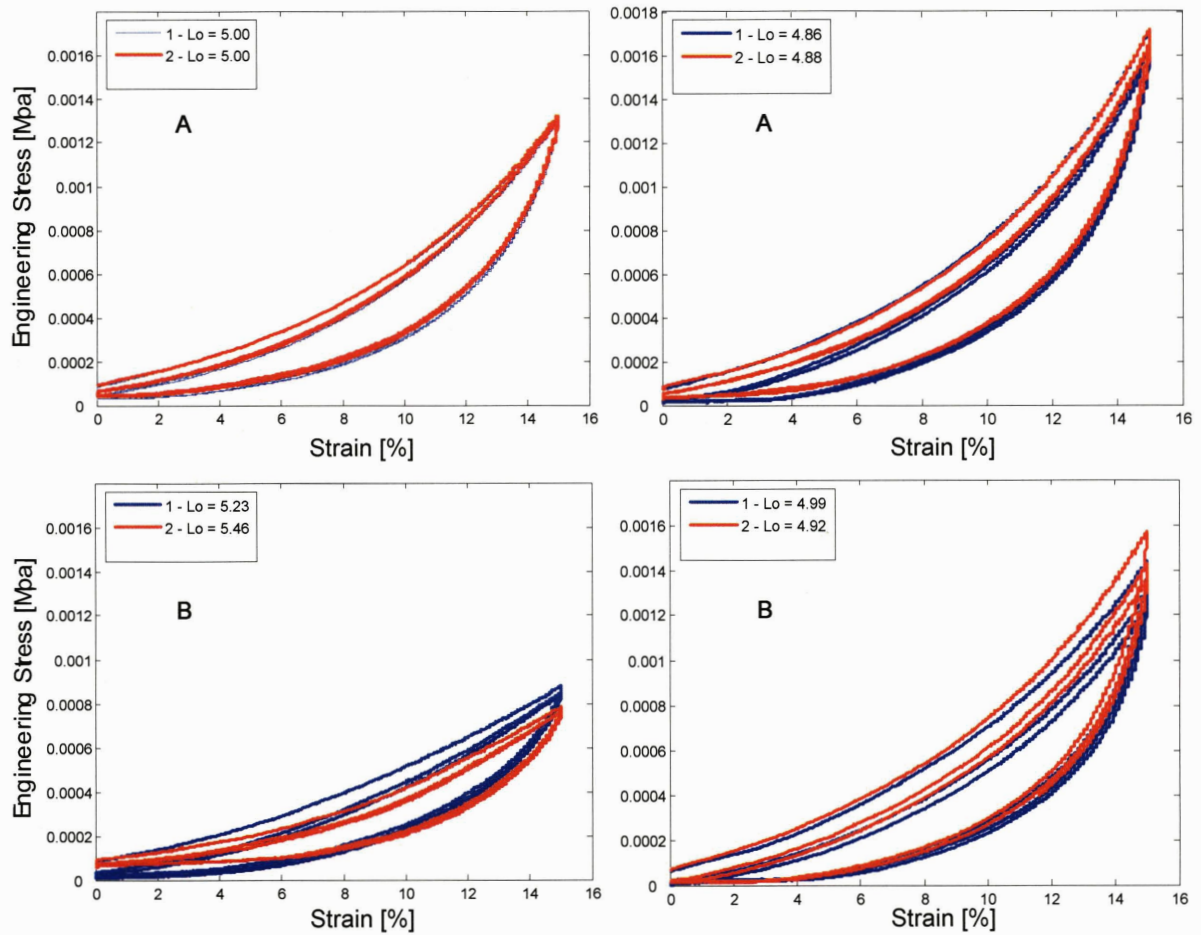
Figure 4-6: Stress Strain response of four samples from cervical slice 1 from a NPPD cervix. A) Sample 1 soaked in saline B) Sample 2 soaked in saline C) Sample 3 soaked in saline and protease inhibitor cocktail D) Sample 4 soaked in saline and protease inhibititor cocktail. Samples soaked in saline as opposed to the saline/protease inhibitor cocktail had more repeatable data.
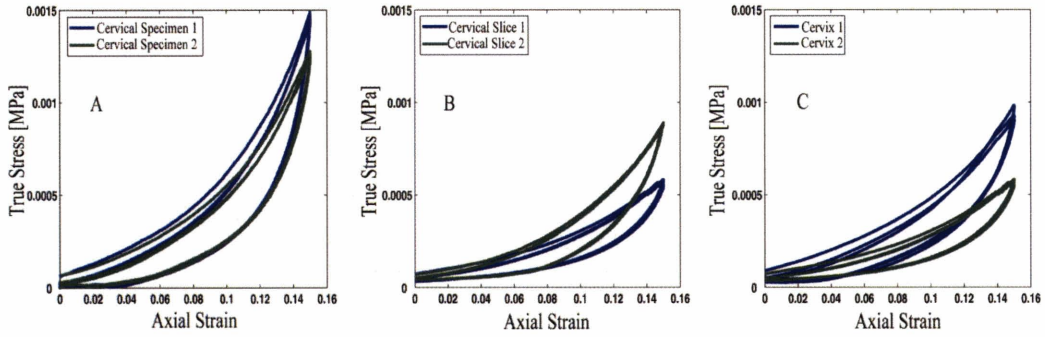
Figure 4-7: Variability in the uniaxial load-unload compression cycle response (A) between two specimens from the same anatomical site for the same cervix; (B) between two specimens from different anatomical site for the same cervix; (C) between two specimens from different cervices.

necessary to uniquely determine the constitutive parameters that characterize the contribution of the collagen network to the tissue response [2]. We therefore introduced an additional testing protocol to evaluate the tensile response of the tissue. In order to reduce sources of variability in the mechanical tissue response, tensile responses and compressive responses will be obtained from adjacent slices. It should be noted that the compression tests were performed with the loading axis parallel to axis of the cervical canal, while the tensile tests should be performed with the loading direction along the circumference of the cervix. Preliminary histological studies were performed on stained stroma samples from human cervices obtained from hysterectomy specimens [18]. We were not able to identify a substantial degree of anisotropy in the arrangement of the collagen bundles; therefore, differences in loading direction are not expected to be significant. However, possible effects of anisotropy on the tissue response are currently under investigation.

Figure 4-8 illustrates the results of the compressive loading protocol on a single tissue specimen. Note the consistent response of the tissue in the load-unload cyclic tests performed before and after the unconfined ramp-relaxation series. Typical re-equilibration times between tests were found to be much shorter (~10 minutes) than the initial equilibration period necessary to prepare the specimen for mechanical testing.
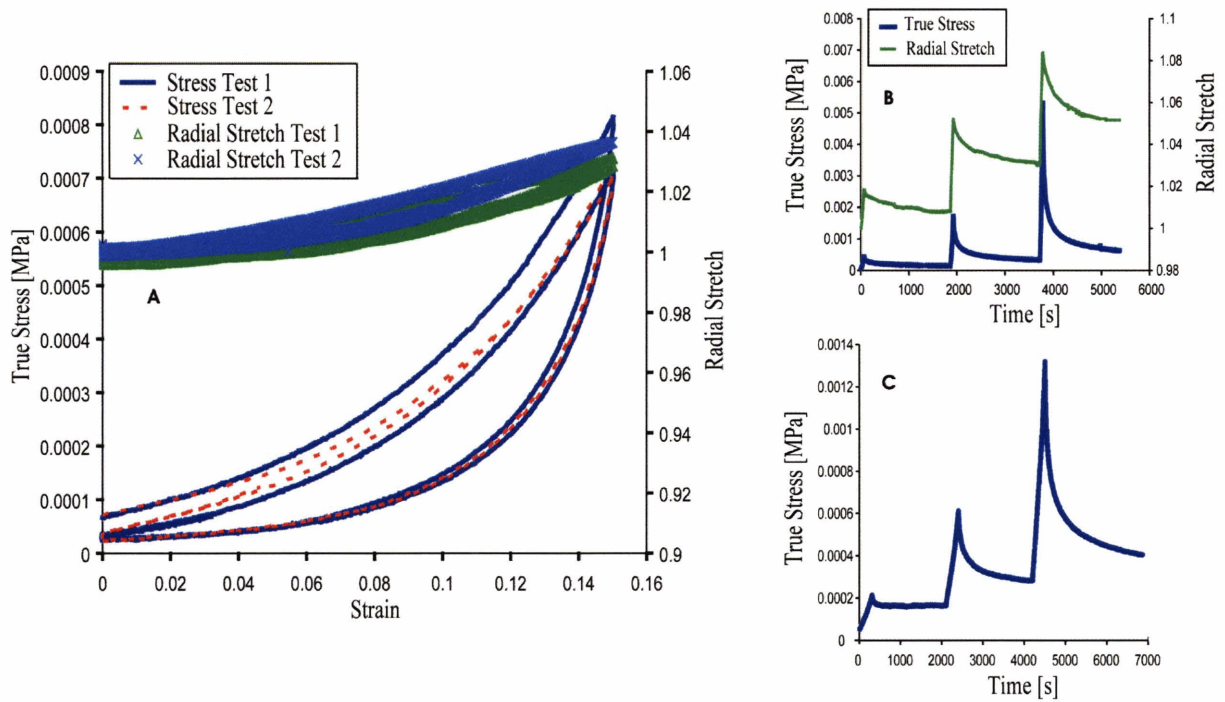
Figure 4-8: Mechanical data collected from a single cervical specimen. (A) True stress and radial stretch measurements from the load-unload compression cycles. Test 1 was conducted before the unconfined ramp-relaxation test and Test 2 was conducted afterwards. (B) True stress and radial stretch measurements from the unconfined ramp-relaxation test. (C) True stress measurements from the confined ramp-relaxation test.

4.1.2 Biochemical Characterization

Homogenization

Homogenization of the cervical tissue was important for reliable and consistent biochemical results. Cervical tissue is extremely fibrous, tense and tough, and it was necessary to break down the tissue for the biochemical assays. The first homogenization technique used by Febvay was to cut the dry cervical tissue into small 10mg pieces using a surgical scalpel [18]. This technique proved to be difficult and did not homogenize the cervical tissue. The collagen content measured with this homogenization technique was underestimated, and the tissue could not digest fully during the proteinase K digestion.

An initial suggestion was to mince the tissue after flash freezing in liquid nitrogen with a large blender, however the cervical samples were too small for the large blades. Instead, the Tissue Tearor by Biospec was recommended because it was designed for smaller tissue samples. The Tissue Tearor was a dremel tool with rotating blades mounted on a thin shaft inside of a thin steel tube (see the website *http://www.biospec.com/Tissue-Tearor.htm* for Tissue Tearor information). The company claimed it pulverizes and lyses tissue in preparation for biochemical assays. However, the Tissue Tearor did not work for the cervical tissue samples. Instead, much of the sample was trapped in the blades and the tissue remained in clumps.

The best method for pulverizing cervical tissue was to crush the frozen tissue in the pre-cooled biopulverizer. This method is outlined in Chapter 2 on Page 51. The crushed tissue should be placed directly into the lyophilizer or a cold extraction solution before the tissue thaws. The most important lessoned learned in pulverization was that the tissue must remain frozen before the start of biochemical assays. If the tissue thaws at any point during the assay, the tissue will clump.

Collagen Content (per Tissue Dry Weight)

Improvements were made in homogenizing the cervical tissue, measuring the tissue dry weight, and digesting the cervical tissue to aid with the collagen analysis. Febvay measured $31.41\pm6.52\%$ collagen content per dry weight in cervical tissue using a protocol intended for articular cartilage [18]. This percentage underestimated cervical collagen content when compared to the

Tissue Preparation for Hydroxyproline Protocol	Collagen Content per dry weight	Error	c = cervices tested n= samples tested
pulverized, pk digest, eppendorf weigh broken lyophilizer	47.2%	±16.3%	c = 3 n = 16
pulverized, HCl digest, eppendorf weigh, broken lyophilizer	59.4%	±8.9%	c = 1 n =4
pulverized, HCl digest, eppendorf weigh Grodzinsky's lyophilizer	77.7%	±8.3%	c = 1 n = 4
pulverized, HCl digest, eppendorf weigh fixed lyophilizer	51.8%	±14.2%	c = 4 n = 14
pulverized, HCl digest, Pyrex weigh fixed lyophilizer	71.6%	±1.8%	c = 1 n = 4

Table 4.1: Collagen content measured from human cervical tissue using the hydroxyproline assay. Different tissue preparations are used to find out which protocol estimates collagen content correctly.

literature [41].

Table 4.1 documents the measured collagen content with each update of the tissue preparation protocol. The first improvement was in the pulverization technique. By completely homogenizing the cervical tissue the measured collagen content improved to 47.2%. The next improvement was the digestion technique. Instead of digesting approximately 4mg of dry tissue in 1ml. of proteinase K solution (0.1mg/ml), the dry tissue was digested in 6N of HCl during the hydrolyzation step. This digestion technique improved the collagen measurement to 59.4%. The last improvement was accurately measuring the tissue dry weight. Instead of measuring the tissue before transferring it to the Pyrex tube, it was measured after transferring. After the measuring improvement, the collagen content measured was 71.6% with an error of ±1.8%.

For an accurate collagen content measurement the following must be taken into consideration: the tissue must be completely homogenized, the dry tissue weight must be accurately measured, the tissue should be digested in 6N HCl , and the tissue must be completely freeze dried to a constant weight.

Collagen Extractability

An initial collagen extraction protocol was adapted from an assay used for rat cervix [39]. This original protocol was tested on two cervical specimens. Negligible amounts of collagen were extracted in the first three extraction solutions containing 0.15M NaCl, 1M NaCl, and 0.5M acetic acid, respectively. These results do not compare to results from the rat cervix experiments.

Because no cervical tissue was solubilized in the initial extraction protocol, a refined extraction protocol was attempted. Cervical tissue was extracted in 0.5M acetic acid without pepsin for 3 days at 4°C. The mixture was then centrifuged for 1 hour at 15,000g and the supernatant and tissue pellet were separated for hydroxyproline analysis. If was found that no collagen was extracted in the 0.5M acetic acid solution. In response, pepsin was added to the extraction solution as recommended by the Petersen extraction method [51]. The addition of pepsin aided in the denaturing of collagen, and as a result human cervical tissue could be solubilized in 0.5M acetic acid with pepsin. The current collagen extraction protocol outlined in Chapter 2 reflect these changes.

Comparison between biochemistry analysis results and literature data

The biochemical measurements reported in the results section are in good agreement with previously reported biochemical results for human cervical tissue. Previous studies by Danforth et al., Petersen et al., and Rechenberger et al. reported significant differences in hydration and collagen extractability between non-pregnant and pregnant tissue samples [11][51][56]. All three investigations report that pregnant tissue is more hydrated than non-pregnant tissue. Furthermore, Petersen et al. concluded that collagen extractability is higher in NPPD tissue as compared to NPND tissue [51]. Rechenberger et al. measured higher collagen extractability in pregnant tissue as compared to non-pregnant tissue [56]. Total collagen content and sulfated glycosaminoglycans measurements also fall within the range of data in the literature. Shimuzu et al. [61] measured 0.75% and 0.97% sulfated glycosaminoglycans per dry weight of tissue for non-pregnant and pregnant tissue, respectively. Petersen et al. [51] measured 94.4% and 73.6% collagen content per dry weight of tissue for NPND and NPPD cervical tissue, respectively.

4.2   Conclusion and Future Work

The mechanical properties of biological tissue can be drastically altered by relatively small modifications in its biochemistry. Nature modulates the mechanical properties of cervical tissue by subtle readjustments of its composition. The compliance of cervical stroma changes by orders of magnitude when the pregnancy nears term. A remarkable change in macroscopic properties is accomplished through subtle shifts in biochemical constituents. The total collagen and GAG contents remain almost unchanged. More significant changes are seen in collagen crosslinking and the relative quantities of sulfated GAGs and hyaluronic acid.

This study represents a first important step towards the attainment of an improved understanding of the complex interplay between the molecular structure of the tissue and its macroscopic mechanical properties. We established mechanical testing and biochemical analysis protocols that will provide the foundation of our investigation of structure-property relations in cervical tissue. Experimental results presented in Chapter 3 indicate that there exists a correlation between obstetric history and biochemical and mechanical properties of the tissue. The results of this study also confirm that higher collagen extractability and hydration levels are associated with more compliant tissue behavior.

Future work will focus on improving the statistical power of this study by significantly increasing the number of tested specimens. More work will also focus on developing tension experiments for cervical tissue and fitting experimental data to a three-dimensional constitutive model.   In a parallel effort, we are developing protocols to quantify the concentrations of distinct glycosaminoglycans by Fluorophore Assisted Carbohydrate Electrophoresis (FACE) [8]. Studies from Osmer et al. [49] and von Maillot et al. [16] investigated the importance of the relative concentrations of different GAGs during pregnancy and labor. It has been shown that the shift in GAG concentration among hyaluronic acid, dermatan sulfate, and the chondroitin sulfates facilitates cervical softening during labor. It has also been shown that the finer structure of the GAG relating to the length of the GAG disaccharide chain and the degree of sulfation is important in the biomechanics of hydrated tissue (e.g. in cornea tissue [52] and osteoarthritic cartilage [53]). Our current DMB assay only measures total sulfated GAG content. The DMB assay does not characterize the electrostatic properties of the distinct GAG chains and cannot measure the hyaluronic acid content. The new FACE assay will allow us to

overcome these limitations and will provide further means to differentiate the biomechanical properties of cervical specimens.

Appendix A

Mechanical and Biochemical Testing Protocols

A.1 Collecting Cervix from the New England Medical Center

A.1.1 Materials

- Stainless steel cervix slicer (Engineering Drawings in Appendix B)

- Multi-Purpose Polyproplene Lab Container (VWR Catalog #15707-950)

- 5mm thick, 1.5" diameter HDPE spacers

A.1.2 Procedure

1. Collect uterus and cervix from operating room and place directly on ice.

2. Bring organ to pathology for inspection and cutting.

3. Cut organ with the stainless steel cervix slice. Place uterus in large well with the cervix resting over the blade indentations. Bring blades down over organ to cut.

4. Place cervical slices on 5mm HDPE spacers and place spacers and cervix in the Polyproplene lab containers. Stack the jars so each cervical slice is sandwiched between two flat surfaces. Careful not to squeeze slice.

5. Place stacked jars in stainless steel thermo-flask with liquid nitrogen and transport organ to MIT. Store cervix at -80°C until time of cutting test specimens.

A.2 Cutting Test Specimens for Mechanical Testing

A.2.1 Materials

- 8mm Miltex disposable biopsy punch (Moore Medical Catalog #52443)

- Surgical scalpel

- Plastic cutting board

- Phosphate Buffered Saline (PBS - 10x VWR Catalog #EM-6508)

- Petry dishes

- Corning 2ml storage vials (VWR Catalog #29442-538)

- Drill press

A.2.2 Procedure

1. Place 8mm biopsy punch in drill press chuck. Make sure biopsy punch is balanced when rotating.

2. Thaw cervical slice in Phosphate Buffered Saline (PBS) for 3 minutes on cutting board.

3. Drill 8mm cores from the stroma of the cervix. Avoid mucosa, facsia, inner canal, and cysts. Keep samples on ice.

4. Cut away 4 small stroma samples adjacent to the site of the 8mm cores (approximately 20mg wet weight). Store in 2ml Corning vials and place into -80°C freezer.

5. Weigh 8mm stroma samples and record wet weight.

6. Store 8mm stroma samples in a petry dish in PBS at 4°C overnight.

A.2.3 Notes

- Do not let biochemistry samples thaw for more than 10 minutes.

- Keep tissue samples on ice.

- Take samples only from stroma region.

A.3 Pulverization and Homogenization for Biochemical Assays

A.3.1 Materials

- Liquid nitrogen

- Thermo-flask

- Alminum foil

- Stainless steel biopulverizer (Engineering Drawings in Appendix B)

- Hammer

- 1.5ml Eppendorf centrifuge tubes (VWR Catalog #20901-551)

A.3.2 Procedure

1. Weigh and label empty 1.5ml centrifuge tubes.

2. Cool biopulverizer for at least 10 minutes in liquid nitrogen.

3. Wrap 20mg of frozen tissue in alminum foil and cool in liquid nitrogen for at least 2 minutes.

4. After 10 minutes of cooling, assemble biopulverizer on lab bench.

5. Remove tissue from liquid nitrogen and aluminum foil and place in the biopulverizer well. Pour small amounts of liquid nitrogen in the well with the tissue.

6. Smash tissue inside biopulverizer well with hammer and pestle.

7. Gently tap out smashed tissue (it will resemble a flat pancake). Place small amounts into preweighed eppendorf tubes. 20mg of tissue can be broken up into 3 1.5ml centrifuge tubes.

8. Weigh tissue in preweighed centrifuge tubes and record wet weight. Place tissue immediately into -80°C freezer for storage.

A.3.3 Notes

- Never let the tissue thaw. Once the tissue thaws, it will stick together.

- Leave tissue in pancake form. It will break into small pieces once vortexed in a cold solution.

- Wear appropriate personal protection for handling liquid nitrogen and human tissue. Wear cryo-safe gloves, lab coat, glasses, and mask.

A.4 Collagen Content - Tissue Preparation for the Hydroxyproline Assay

A.4.1 Materials and Equipment

- Pyrex Culture Test Tubes with Teflon Resin-Faced Rubber-Lined Caps (VWR Catalog #60827-533)

- lyophilizer (Labconoco 4.5 Liter)

- 6N Hydrochloric Acid (HCl)

- Spectrophotometer

A.4.2 Procedure

1. Pulverize tissue sample, weigh, and keep frozen at -80°C.

2. Freeze dry frozen pulverized tissue overnight.

3. Weigh and label empty Pyrex test tubes.

4. Place freeze dried tissue in preweighed Pyrex tubes. Weigh tissue dry weight.

5. Add 1ml of 6N HCl to each sample and vortex.

6. Place samples in oven at 115°C overnight for hydrolyzation.

7. After hydrolyzation, follow standard hydroxyproline assay. Read absorbency at 560nm in the spectrophotometer.

A.5   Collagen Extractability

A.5.1   Equipment and Materials

- Glacial Acetic Acid

- Pepsin

- 1.5ml Eppendorf centrifuge tubes

- laboratory rocker

- centrifuge

- Spectrophotometer

A.5.2   Procedure

1. Pulverize tissue sample, weigh, and keep frozen at -80°C.

2. Make acetic acid extraction solution (150μl/mg of wet tissue). Dilute Glacial Acetic Acid (17M) to 0.5M with deionized water. Dissolve 1mg/ml of pepsin into 0.5M acetic acid. Vortex solution and keep on ice.

3. Add acetic acid/pepsin extraction solution to frozen pulverized tissue (150μl/mg of wet tissue) and vortex. Tissue pancake should break into small pieces.

4. Place samples on lab rocker in 4°C refrigerator for 3 days.

5. Weigh and label empty 1.5ml centrifuge tubes for extraction supernatant storage.

6. After 3 days of extracting, centrifuge samples at 15,000g for 1 hour.

7. Separate supernatant and tissue pellet. Pipette supernatant into separate 1.5ml pre-weighed eppendorf tube. Store supernatant at -80°C.

8. Store tissue pellet at -80°C.

9. Freeze dry supernatant and tissue pellet overnight.

10. Add 6N HCl to samples and transfer to Pyrex test tubes for hydrolyzation.

11. Follow hydroxyproline assay to calculate collagen content of each test tube. Read absorbency at 560nm in the spectrophotometer.

12. The total collagen content for the sample is the sum of the collagen content measured in the acetic acid supernatant and the tissue pellet.

13. The acetic acid fraction is calculated as the collagen content measured in the acetic acid supernatant divided by the total measured collagen content.

A.6   Sulfated Glycosaminoglycan Content - DMMB assay

A.6.1   Materials

- water bath

- lyophilizer (Labconoco 4.5 Liter)

- proteinase K (Roche Applied Science)

- Dimethylmethylene blue dye (Polyscience INC.)

- Molecular Devices micro-array spectrophotometer

A.6.2 Procedure

1. Pulverize tissue sample, weigh, and keep frozen at -80°C.

2. Freeze dry frozen tissue overnight.

3. Weigh tissue dry weight.

4. Add 1ml of proteinase k solution (0.1mg/ml) to each sample.

5. Incubate samples in a 60°C water bath for 24 hours.

6. Place samples in a 100°C water bath for 10 minutes to stop proteinase K digest.

7. For the DMMB assay, place $20\mu l$ of digested tissue into micro plate wells with $200\mu l$ of DMB dye.

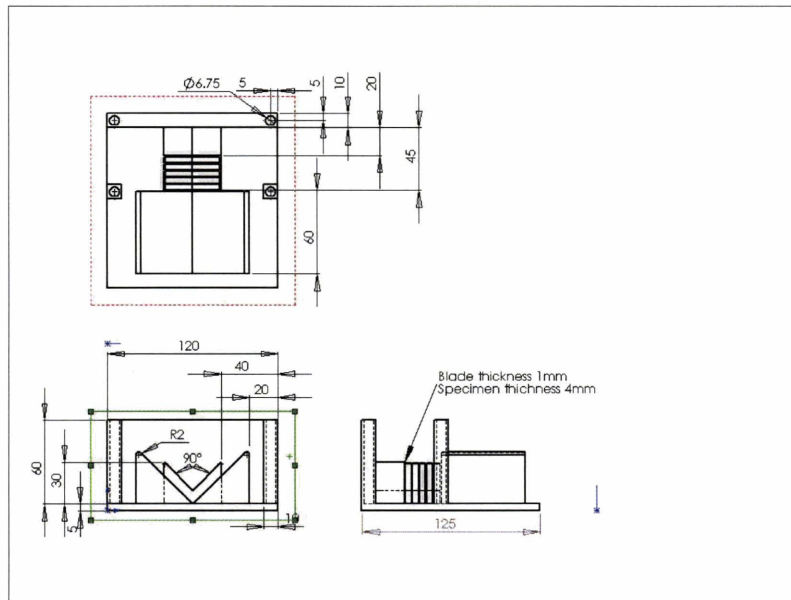8. Read absorbency at 520nm in the spectrophotometer.

Appendix B

Engineering Drawings (all dimensions in mm)
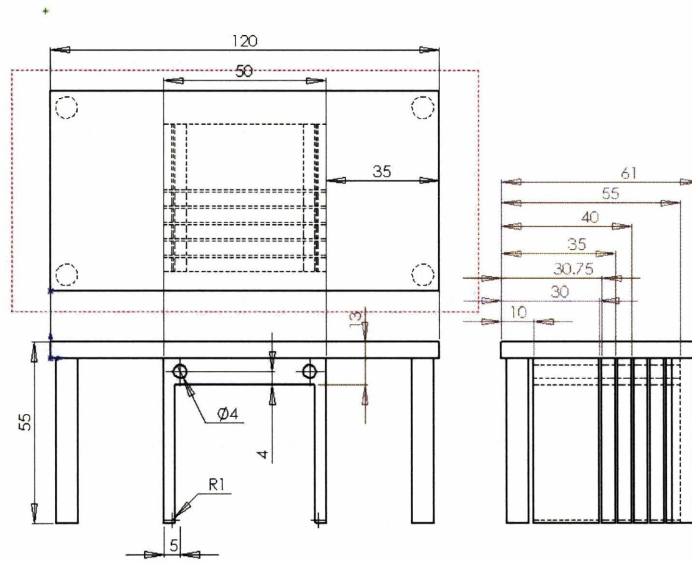
B.1   Cervix Slicer
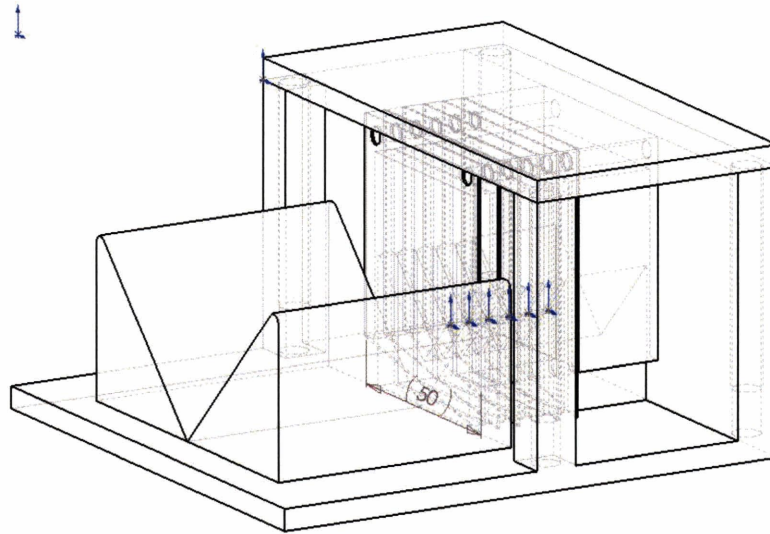
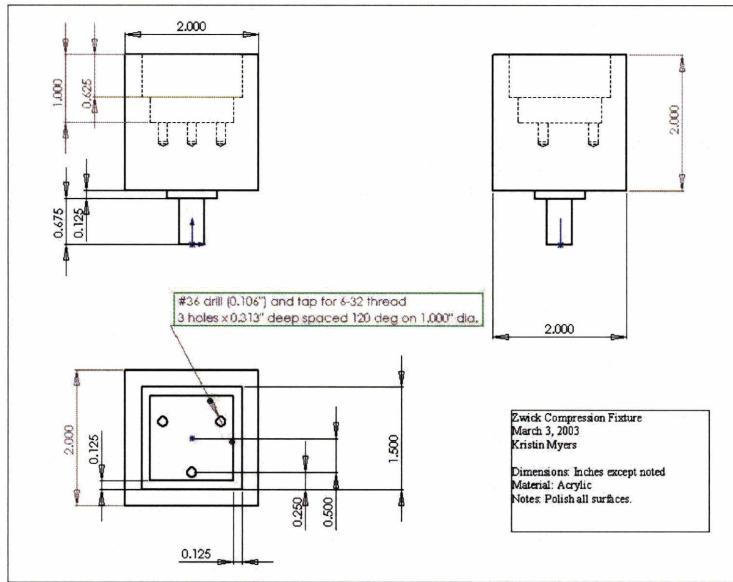Assembly drawing of the cervical slicer

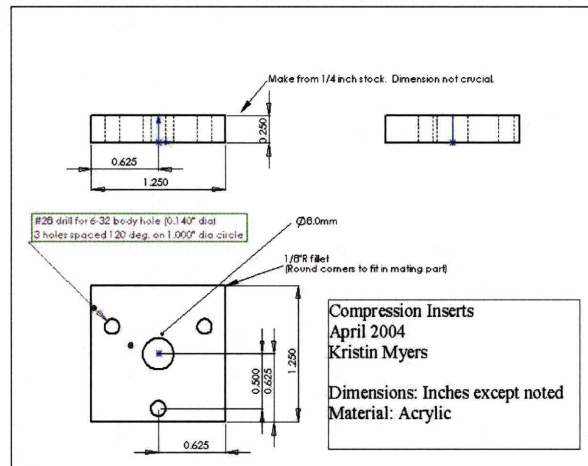Bottom of the cervical slicer

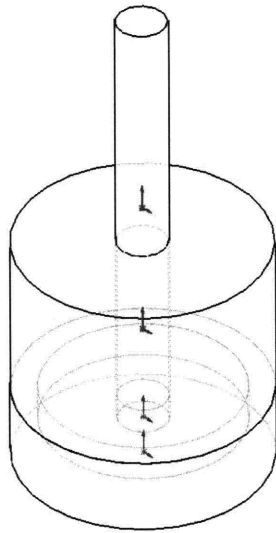Top of the cervical slicer

B.2   Compression Fixture

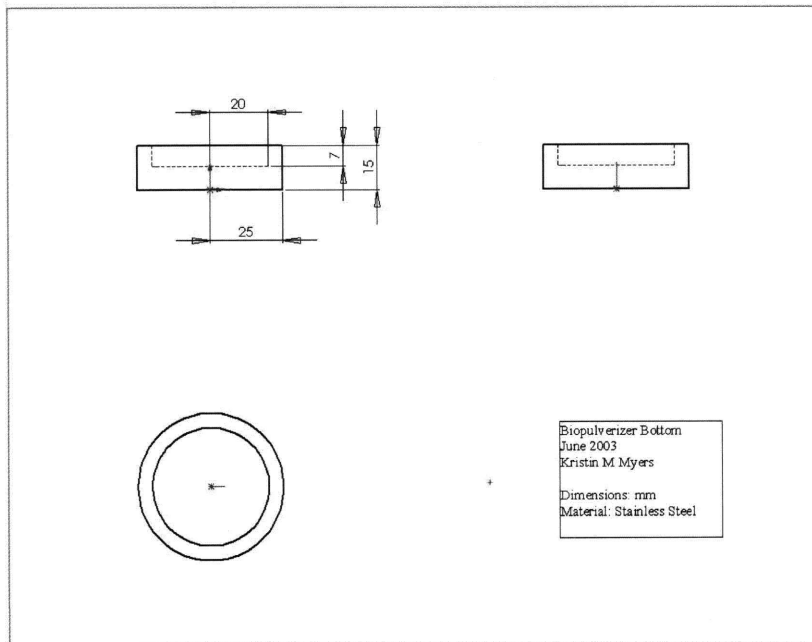Fixture for mechanical tests

Fixture inserts for confined ramp-relaxation tests

B.3 Biopulverizer

Assembly view of the biopulverizer.

20

7

15

25

Biopulverizer Bottom
June 2003
Kristin M Myers

Dimensions: mm
Material: Stainless Steel
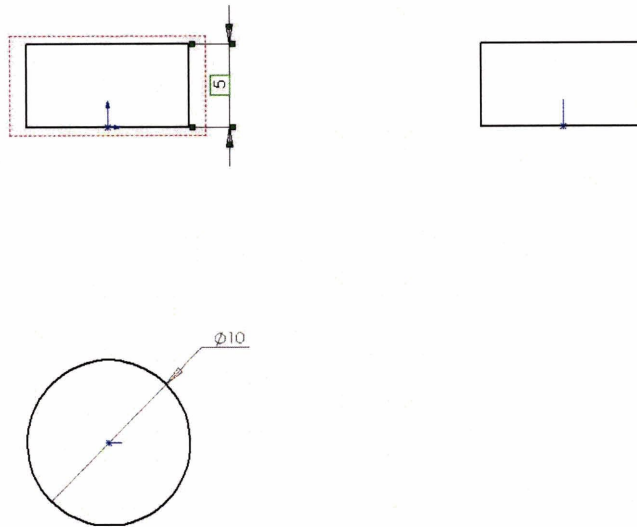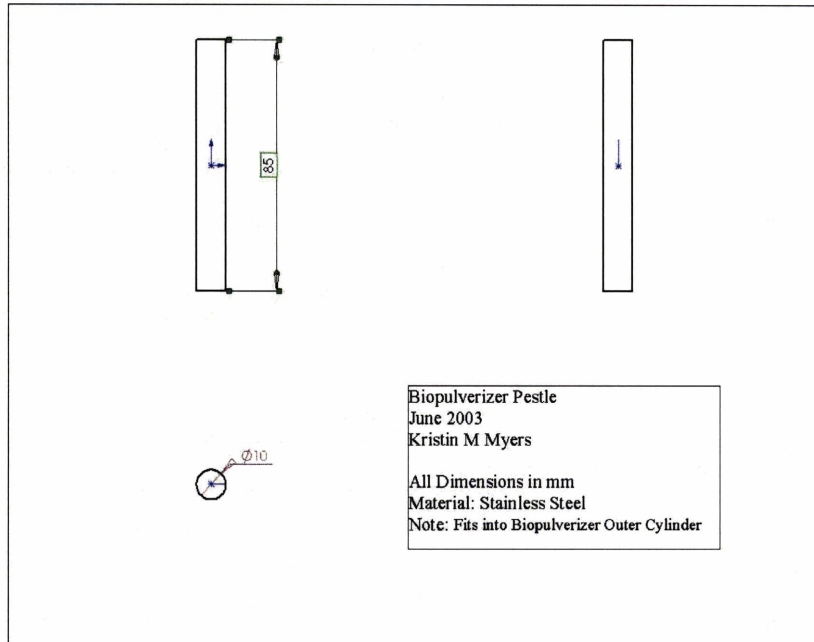
Bottom of the biopulverizer
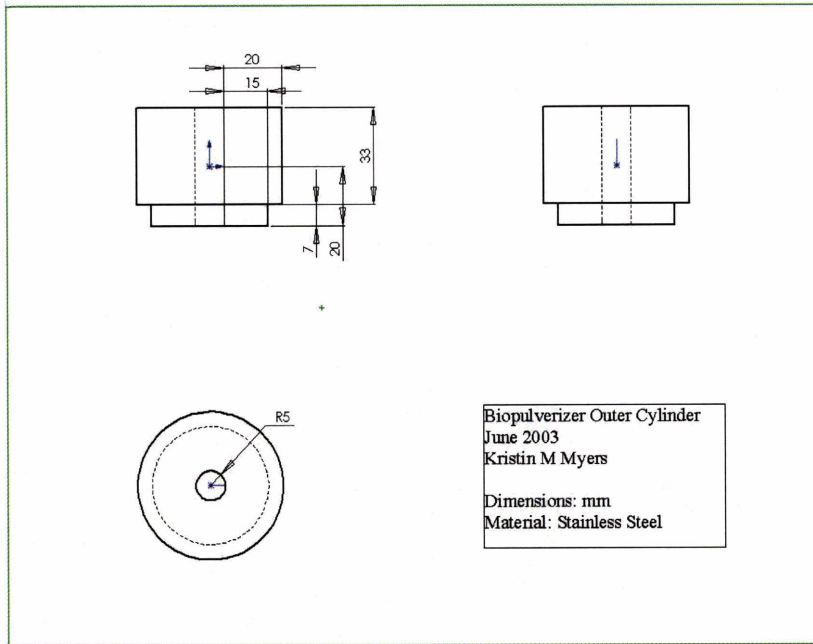
Top cylinder of the biopulverizer.

Inner cylinder of the biopulverizer

Biopulverizer Pestle
June 2003
Kristin M Myers

All Dimensions in mm
Material: Stainless Steel
Note: Fits into Biopulverizer Outer Cylinder

Biopulverizer pestle

Bibliography

[1] S.M. Althuisius, G.A. Dekker, P. Hummel, D.J. Bekedam, and H.P. van Geijn. Final results of the cervical incompetence prevention randomized cerclage trial (cipract): Therapeutic cerclage with bed rest versus bed rest alone. *Am J Obstet Gynecol*, 185(5):1106–1112, November 2001.

[2] R.M. Aspden. The theory of fibre-reinforced composite materials applied to changes in the mechanical properties of the cervix during pregnancy. *J Theor Biol.*, 130(2):213–221, 1988.

[3] Peter J. Basser, Rosa Schneiderman, Ruud A. Bank, Ellen Wachtel, and Alice Maroudas. Mechanical properties of the collagen network in human articular cartilage as measured by osmotic stress technique. *Archives of Biochemistry and Biophysics*, 351(2):207–219, March 1995.

[4] V. Berghella, S.F. Daly, J.E. Tolosa, M.M. Divito, R. Chalmers, and N. Garg. Prediction of preterm delivery with transvaginal ultrasonography of the cervix in patients with high-risk pregnancies: does cerclage prevent prematurity? *Am J Obstet Gynecol*, 181:809–815, 1999.

[5] D.W. Branch. Operations for cervical incompetence. *Clin Obstet Gynecol*, 1986.

[6] Neil D. Broom and Anthony Poole. Articular cartilage collagen and proteoglycans: Their functional interdependency. *Arthritis and Rheumatism*, 26(9), September 1983.

[7] Neil D. Broom and Heather Silyn-Roberts. The three-dimensional 'knit' of collagen fibrils in articular cartilage. *Connective Tissue Research*, 23:261–277, 1989.

[8] A Calabro, V.C. Hascall, and R.J. Midura. Adaptation of face methodology for microanalysis of total hyaluronan and chondroitin sulfate composition from cartilage. *Glycobiology*, 10(3):283–293, 2000.

[9] John T. Conrad, Richard D. Tokarz, and John F. Williford. *Dilatation of thet Uterine Cervix: Connective Tissue Biology and Clincial Managemen*, chapter 18 Anatomic Site and Stretch Modulus in the Human Cervix, pages 255–264. Raven Press, 1980.

[10] Robert K. Creasy and Robert Resnik. *Maternal-Fetal Medicine*, chapter 29. W.B. Saunders Company, 4 edition, 1984.

[11] D.N. Danforth, A. Veis, M. Breen, H.G. Weinstein, J.C. Buckingham, and P. Manalo. The effect of pregnancy and labor on the human cervix: Changes in collagen, glycoproteins, and glycosaminoglycans. *Am J Obstet Gynecol*, 120(3):641–651, November 1974.

[12] K.G. Danielson, H. Baribault, D.F. Holmes, H. Graham, K.E. Kadler, and V. Iozzo. Targeted disruption of decorin leads to abnormal collagen fibril morphology and skin fragility. *J of Cell Bio*, 136(3):729–743, February 1997.

[13] James Darnel, Harvey Lodish, and David Baltimore. *Molecular Cell Biology*, chapter 23. Scientific American Books, 2 edition, 1990.

[14] Solomon R. Eisenberg and Alan J. Grodzinsky. Swelling of articular cartilage and other connective tissues: Electromechanochemical forces. *J Orthop Res*, 1985.

[15] G. Ekman, H. Almstrom, L. Granstrom, A. Malmstrom, M. Norman, and Jr J.F. Woessner. *The Extracellular Matrix of the Uterus, Cervix and Fetal Membranes: Synehesis, Degradation and Hormonal Regulation*, chapter 8 Connective tissue in human cervical ripening. Perinatology Press, 1991.

[16] Ellwood, editor. *The Cervix in Pregnancy and Labour: Clinical and Biochemical Investigations. Connective tissue changes in the human cervix in pregnancy and labour*, chapter 23 Determination of Hydroxyproline in Connective Tissues. Churchill Linvingston INC, New York, 1981.

[17] Richard W. Farndale, Christine A. Sayers, and Alan J. Barrett. A direct spectrophoto-metric microassay for sulfated glycosaminoglycans in cartilage cultures. *Connective Tissue Research*, 9:247–248, 1982.

[18] S. Febvay. A three-dimensional constitutive model for the mechanical behavior of cervical tissue. Master's thesis, Massachusetts Institute of Technology, 2003.

[19] R.E. Garfield, G. Saade, C. Buhimschi, I. Buhimschi, L. Shi, S-Q. Shi, and K. Chwalisz. Control and assessment of the uterus and cervix during pregnancy and labour. *Human Reproduction Update*, 4(5):673–695, 1998.

[20] K. Gelse, E. Poschl, and T. Aigner. Collagens-structure, function, and biosynethesis. *Advanced Drug Delivery Reviews*, 55:1531–1546, 2003.

[21] R.L. Goldenberg, J.D. Iams, B.M. Mercer, P. Meis, A. Moawad, A. Das, R. Cooper, and F. Johnson. What we have learned about the predictors of preterm birth. *Semin Perinatol*, 27(3):185–193, 2003.

[22] E.R. Guzman, R. Mellon, A.M. Vintzileos, C.V. Ananth, C. Walters, and K. Gipson. Relationship between endocervical canal length between 15-24 weeks gestation and obsteric history. *J of Maternal-Fetal Med*, 7:269–272, 1998.

[23] E.R. Guzman, C. Walters, C. V. Ananth, C. O'Reilly-Green, C.W. Benito, A. Palermo, and A.M. Vintzileos. A comparison of sonogrpahic cervical parameters in predicting spon-taneous preterm birth in high-risk singleton gestations. *Ultrasound Obstet Gynecol*, 18:204–210, 2001.

[24] Margaret L. R. Harkness and R.D. Harkness. Changes in the physical properties of the uterine cervix of the rat during pregnancy. *J. Physiol.*, 148:524–547, 1959.

[25] R. Harrison, R. Iozzo, and I. Weber. Model structure of decorin and implication for collagen fibrillogenesis. *J of Bio Chem*, 271(50):31767–31770, 1996.

[26] V.C. Heath, A.P. Souka, I. Erasmus, D.M. Gibb, and K.H. Nicolaides. Cervical length at 23 weeks of gestation: the value of shirodkar suture for the short cervix. *Ultrasound Obstet Gynecol*, 12:318–322, 1998.

[27] D. Heinegard, V. Hascall, and T. Wight. *Cell Biology of Extracellular Matrix*, chapter 2 Proteoglycans Structure and Function. Plenum Press, 1991.

[28] J.U. Hibbard, J. Snow, and A.H. Moawad. Short cervical length by ultrasound and cerclage. *J Perinatol*, 20:161–165, 2000.

[29] A.M. Hocking, T. Shinomura, and D. McQuillan. Leucine-rich glycoproteins of the extracellular matrix. *Matrix Biology*, 17:1–19, 1998.

[30] Caroline D. Hoemann, Jun Sun, Veronica Chrzanowski, and Micheal Bushmann. A multivalen assay to detect glycosaminoglycan, protein, collagen, rna, and dna content in milligram samples of cartilage or hydrogel-based repair cartilage. *Analytical Biochemistry*, 300(1-10), 2002.

[31] J.D. Iams, F.F Johnson, J. Sonek, L Sachs, C. Gebauer, and P. Samuels. Cervical competence as a continuum: A study of ultrasonographic cervical length and obstetric performance. *A J of Obstet Gyn*, 142(4):1097–1106, April 1995.

[32] A. Ito, Y. Mori, and S. Hirakawa. Purification and characterization of an acid proteinase from human uterine cervix. *Chem. Pharm. Bull*, 27:969–973, 1979.

[33] J.F. Woessner Jr. *Methodology of Connective Tissue Research*, chapter 23 Determination of Hydroxyproline in Connective Tissues. Joynson-Bruvvers Ltd., Oxford, 1976.

[34] D.R. Keene, J.D. San Antonia, R. Mayne, D.J. McQuillan, G. Sarris, S.A. Santoro, and R.V. Iozzo. Decorin binds near the c terminus of type 1 collagen. *J of Bio Chem*, 257(29):21801–21804, 2000.

[35] GN Kiefer, K Sundby, D McAllister, NG Shrive, CB Frank, T Lam, and NS Schachar. The effect of cryopreservation on the biomechanical behavior of bovine articular cartilage. *J Orthop Res*, 7(4):494–501, 1989.

[36] Robert Kiwi, Michael R. Neuman, Irwin R. Merkatz, Mostafa A. Selim, and Andrzej Lysikiewicz. Determination of the elastic properties of the cervix. *Obsterics and Gynecology*, 71(4):568–574, April 1988.

[37] H.P. Kleissl, Michel Van Der Rest, Frederick Naftolin, Francis H. Glorieux, and Alberto De Leon. Collagen changes in the human uterine cervix at parturition. *Am. J. Obstet. Gynecol.*, 130(7):748–753, 1978.

[38] Robert Kokenyesi. *The Extracellular Matrix of the Uterus, Cervix and Fetal Membranes: Synehesis, Degradation and Hormonal Regulation*, chapter 2 Collagen and proteoglycans. Perinatology Press, 1991.

[39] Robert Kokenyesi, Lucas C. Armstrong, Azin Agah, Raul Artal, and Paul Bornstein. Thrombospondin 2 deficiency in pregnant mice results in premature softening of the uterine cervix. *Biology of Reproduction*, 70:385–390, 2004.

[40] Robert Kokenyesi and Jr. J. Frederick Woessner. Relationship between dilatation of the rat uterine cervix and a small dermatan sulfate proteoglycan. *Biology of Reproduction*, 1990.

[41] P.C. Leppert and S.Y. YU. Three dimensional structures of uterine elastic fibers. *Conn. Tissue Res.*, 27:15–31, 1991.

[42] Phyllis C. Leppert. Cervical softening, effacement, and dilatation: A complex biochemical cascade. *The Journal of Maternal-Fetal Medicine*, 1:213–223, 1992.

[43] Phyllis C. Leppert. Anatomy and physiology of cervical ripening. *Clinical Obstetrics and Gynecology*, 38(2):267–279, 1995.

[44] Phyllis C. Leppert, Robert Kokenyesi, Crhistine A. Lemenich, and John Fisher. Further evidence of a decorin-collagen interaction in the disruption of cervical collagen fibers during rat gestation. *Am J Obstet Gyncol*, 182(4):805–812, April 2000.

[45] Phyllis C. Leppert and Shiu Yeh Yu. *The Extracellular Matrix of the Uterus, Cervix and Fetal Membranes: Synehesis, Degradation and Hormonal Regulation*, chapter 6 The collageneous tissue of the cervix during pregnancy and delivery. Perinatology Press, 1991.

[46] Emad El Maradny, Noahiro Kanayama, Hiroshi Kobayashi, Belayet Hossain, Selina Khatun, She Liping, Takao Kobayashi, and Toshihiko Terao. The role of hyaluronic acid

as a mediator and regulator of cervical ripening. *Human Reproduction*, 2(5):1080–1088, 1997.

[47] P.D. Marx. Transabdominal cervicoisthmic cerclage: a review. *Obstet Gynecol Surv.*, 44(7):518–522, 1989.

[48] Hideaki Nagase. *The Extracellular Matrix of the Uterus, Cervix and Fetal Membranes: Synehesis, Degradation and Hormonal Regulation*, chapter 3 Matrix metalloproteinases 1, 2, and 3: substrate specificities. Perinatology Press, 1991.

[49] R Osmers, W Rath, MA Pflanz, W Kuhn, HW Stuhlsatz, and M Szeverenyi. Glycosaminoglycans in cervical connective tissue during pregnancy and parturition. *Obstet Gynecol*, 81:88–92, 1993.

[50] Michelle L. Oyen, Steven E. Calvin, and Robert F. Cook. Uniaxial stress-relaxation and stress-strain responses of human amnion. *Journal of Material Science: Materials in Medicine*, 15:619–624, 2004.

[51] Lone K. Petersen and Niels Uldbjerg. Cervical collagen in non-pregnant women with previous cervical incompetence. *Europ J Obstet Gynec Repr Bio*, 67:41–45, 1996.

[52] AH Plaas, LA West, EJA Thonar, AZ Karcioglu, CJ Smith, GK Klintworth, and VC Hascall. Altered fine structures of corneal and skeletal keratin sulfate and chondroitin/dermatan sulfate in macular corneal dystrophy. *J Biol Chem*, 276(43):39788–39796, 2001.

[53] AH Plaas, LA West, S Wong-Palms, and FR Nelson. Glycosaminoglycan sulfation in human osteoarthritis. *J Biol Chem*, 273(20):12642–12649, 1998.

[54] W. Rath, R. Osmers, M. Severenyi, H.W. Stuhlsatz, and W. Kuhn. *The Extracellular Matrix of the Uterus, Cervix and Fetal Membranes: Synehesis, Degradation and Hormonal Regulation*, chapter 10 Changes of glycosaminoglycans in cervical connective tissue. Perinatology Press, 1991.

[55] T. Rechberger and N. Uldbjerg. Connective tissue changes in the cervix during normal pregnancy and pregnancy complicated by cervical incompetence. *Obstet Gynecol*, 71:563–567, 1988.

[56] T Rechenberger, N Uldbjerg, and H Oxlund. Connective tissue changes in the cervix during normal pregnancy and pregnancy complicated by cervical incompetence. *Obstet Gynecol*, 71:563–567, 1988.

[57] J.M. Rennie. Perinatal management at the lower margin of viability. *Arch Dis Child*, 74:F214–18, 1996.

[58] O.A. Rust, R.O Atlas, J. Reed, J. van Gaalen, and J. Balducci. Revisiting the short cervix detected by transvaginal ultrasound in the second trimester: Why cerclage therapy may not help. *Am J Obstet Gynecol*, 185(5):1098–1105, November 2001.

[59] Maria B. Sennstrom, Gunvor Ekman, Gunilla Westergren-Thorsson, Anders Malmstrom, Birgitta Bystrom, Ursula Endresen, Nokwanda Mlambo, Margareta Norman, Berit Stabi, and Annelie Brauner. Human cervical ripening, an inflammatory process mediated by cytokines. *Molecular Human Reproduction*, 6(4):375–381, 2000.

[60] Maria B. Sensstrom, Annelie Brauner, Birgitta Bystrom, Anders Malmstrom, and Gunvor Ekman. Matrix metalloproteinase-8 correlates with the cervical ripening process in humans. *Acta Obstetricia et Gynecologica Scandinavica*, 2003.

[61] Takeo Shimizu, Masahiko Endo, and Zensaku Yosizawa. Glycoconjugates (glycosaminoglycans and glycoproteins) and glycogen in the human cervix uteri. *Tohoku J. exp. Med.*, 131:289–299, 1980.

[62] H Stegeman and K Stalder. Determination of hydroxyproline. *Clin Chem Acta*, 18:267–273, 1967.

[63] Stanley J. Stys, William H. Clewell, and Giacomo Meschia. Changes in cervical compliance at parturition independent of uterine activity. *American Journal of Obsterics and Gynecology*, 130(4):414–418, February 1978.